Geochemistry Geophysics Geosystems G3
AN ELECTRONIC JOURNAL OF THE EARTH SCIENCES
Published by AGU and the Geochemical Society

Data Brief
Volume 5, Number 7
30 July 2004
Q07004, doi:10.1029/2003GC000684
ISSN: 1525-2027

Gravity, magnetic, and high-precision relocated seismicity profiles suggest a connection between the Hayward and Calaveras Faults, northern California

D. A. Ponce, R. W. Simpson, R. W. Graymer, and R. C. Jachens
U.S. Geological Survey, 345 Middlefield Road, Menlo Park, California 94025, USA (ponce@usgs.gov; simpson@usgs.gov; rgraymer@usgs.gov; jachens@usgs.gov)

[1] Gravity, magnetic, and seismicity data profiled across the Hayward Fault Zone were generated as part of ongoing studies to help determine the geologic and tectonic setting of the San Francisco Bay region. These data, combined with previous geophysical studies that indicate that the Hayward Fault Zone dips 75°NE near San Leandro and follows a preexisting structure, reveal a possible direct connection between the seismogenic portion of the Hayward and Calaveras Faults at depth. Although the relocated seismicity data are regional in nature, they suggest that the dip of the Hayward Fault Zone may vary from near vertical in the northwestern part of the fault to about 75°NE at San Leandro in the central part of the fault to about 50°NE in the southeastern part of the fault. Gravity and magnetic data, profiled across the Hayward Fault Zone, were processed using standard geophysical techniques. Cross sections of high-precision relocated hypocenters were constructed along each profile from the northwestern to the southeastern end of the Hayward Fault Zone. Profiles and cross sections are referenced to Pinole Point, where the Hayward Fault enters San Pablo Bay, and are spaced 2.5 km apart. Topographic profiles shown on the seismicity cross sections were generated using U.S. Geological Survey (USGS) 7.5-min, 30-m digital elevation models. Relocation of seismicity data was accomplished using a regional double-difference method. The double-difference method incorporates ordinary travel time measurements and cross correlation of *P* and *S* wave differential travel time measurements. Relative locations between earthquakes have hypocentral errors of about 100 m horizontally and 250 m vertically. Absolute location uncertainties were not determined but are probably dramatically improved compared to the USGS's Northern California Seismic Network catalog data.

Components: 4438 words, 34 figures, 1 table, 1 dataset.

Keywords: seismicity; gravity; magnetics; Hayward Fault; California.

Index Terms: 1219 Geodesy and Gravity: Local gravity anomalies and crustal structure; 1517 Geomagnetism and Paleomagnetism: Magnetic anomaly modeling; 7230 Seismology: Seismicity and seismotectonics.

Received 22 December 2003; **Revised** 5 April 2004; **Accepted** 24 May 2004; **Published** 30 July 2004.

Ponce, D. A., R. W. Simpson, R. W. Graymer, and R. C. Jachens (2004), Gravity, magnetic, and high-precision relocated seismicity profiles suggest a connection between the Hayward and Calaveras Faults, northern California, *Geochem. Geophys. Geosyst.*, *5*, Q07004, doi:10.1029/2003GC000684.

1. Introduction

[2] Gravity and magnetic profiles, and seismicity cross sections across the Hayward Fault Zone were generated as part of ongoing studies to help determine the geologic and tectonic setting of the San Francisco Bay region and aid in the determination of the earthquake hazard potential of the Hayward Fault. The Hayward Fault itself is enigmatic, in that it creeps at the surface, but is also capable of producing large earthquakes [e.g., *Bürgmann et al.*, 2000; *Lienkaemper et al.*, 1991; *Simpson*,

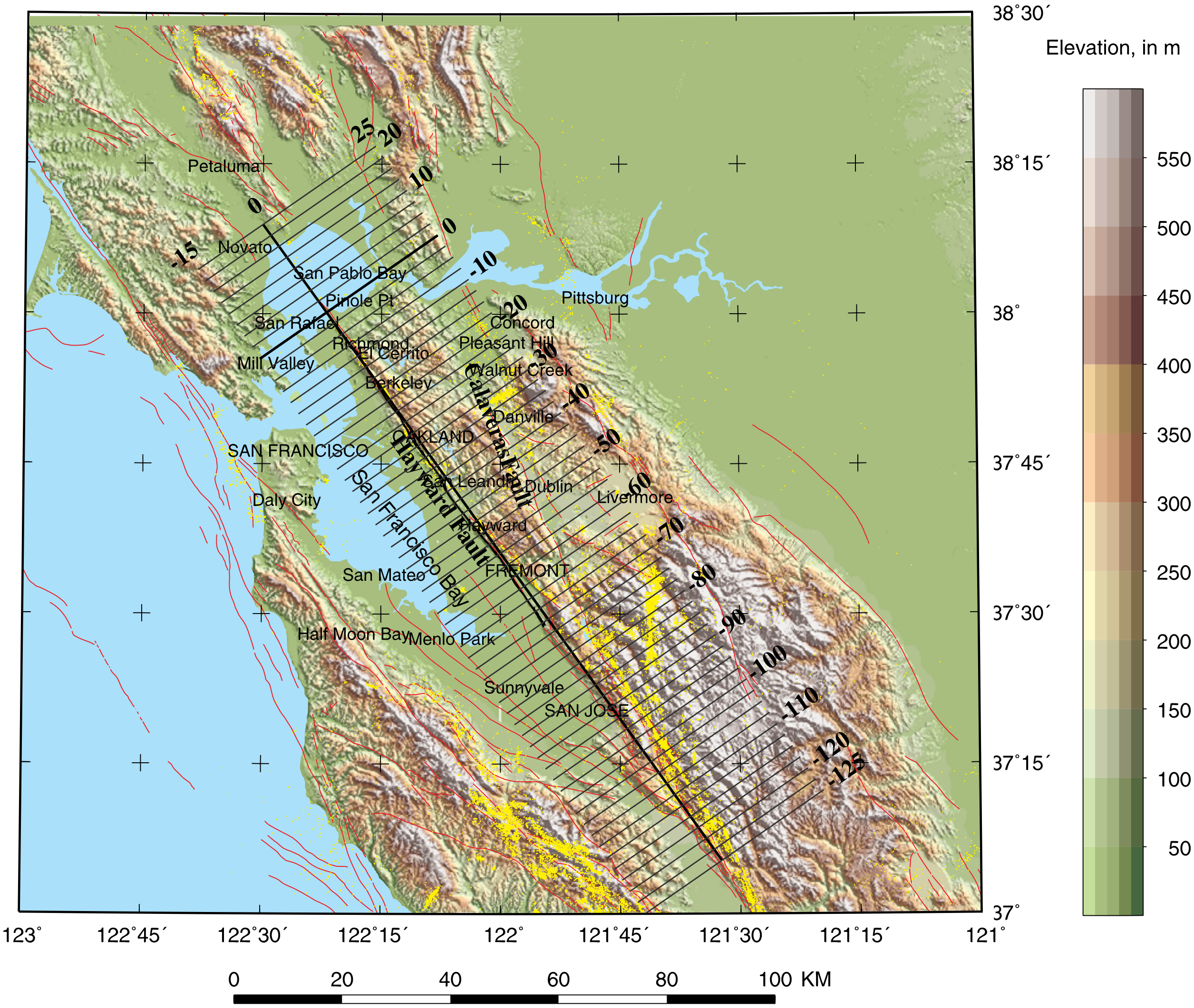

Figure 1. Index and topographic map of the Hayward Fault and vicinity showing location of profiles (distances in kilometers). Black line, recent trace of Hayward Fault from *Lienkaemper et al.* [1991]; red lines, faults from *Jennings et al.* [1977]; yellow triangle, relocated double-difference seismicity from 1984 to 2000.

2000]. The Hayward Fault and its northern extension, the Rodgers Creek Fault, are regarded as one of the most hazardous fault systems in the San Francisco Bay Area with a future probability for a $\geq M6.7$ earthquake of about 27% over the next thirty years [e.g., *Working Group on California Earthquake Probabilities*, 1999, 2003]. Including the southern extension, the Hayward Fault extends for more than about 100 km from San Pablo Bay in the northwest to San Jose in the southeast (Figure 1).

[3] The Hayward Fault is predominantly a right-lateral strike-slip fault that forms the western boundary of the East Bay Hills, but also exhibits modest transpressional motion. Recently, *Graymer et al.* [2002] and *Graymer* [2003] suggested that there may be about 100 km of strike-slip offset on the Hayward Fault on the basis of the restoration of post-12 Ma offset of Miocene volcanic and other rocks. Active right-lateral slip on the Hayward Fault is evidenced by creep on offset natural and man-made features, surface geodetic network measurements, and an $M6.8$ earthquake in 1868.

[4] The Hayward Fault Zone separates two diverse basement terranes from one another: Franciscan Complex rocks (composed predominantly of highly sheared graywacke and basalt interleaved in a mélange of argillite and mixed blocks) on the southwest, and Jurassic Coast Range ophiolite and Jurassic and Cretaceous Great Valley Sequence rocks (clastic submarine fan and basin deposits) on

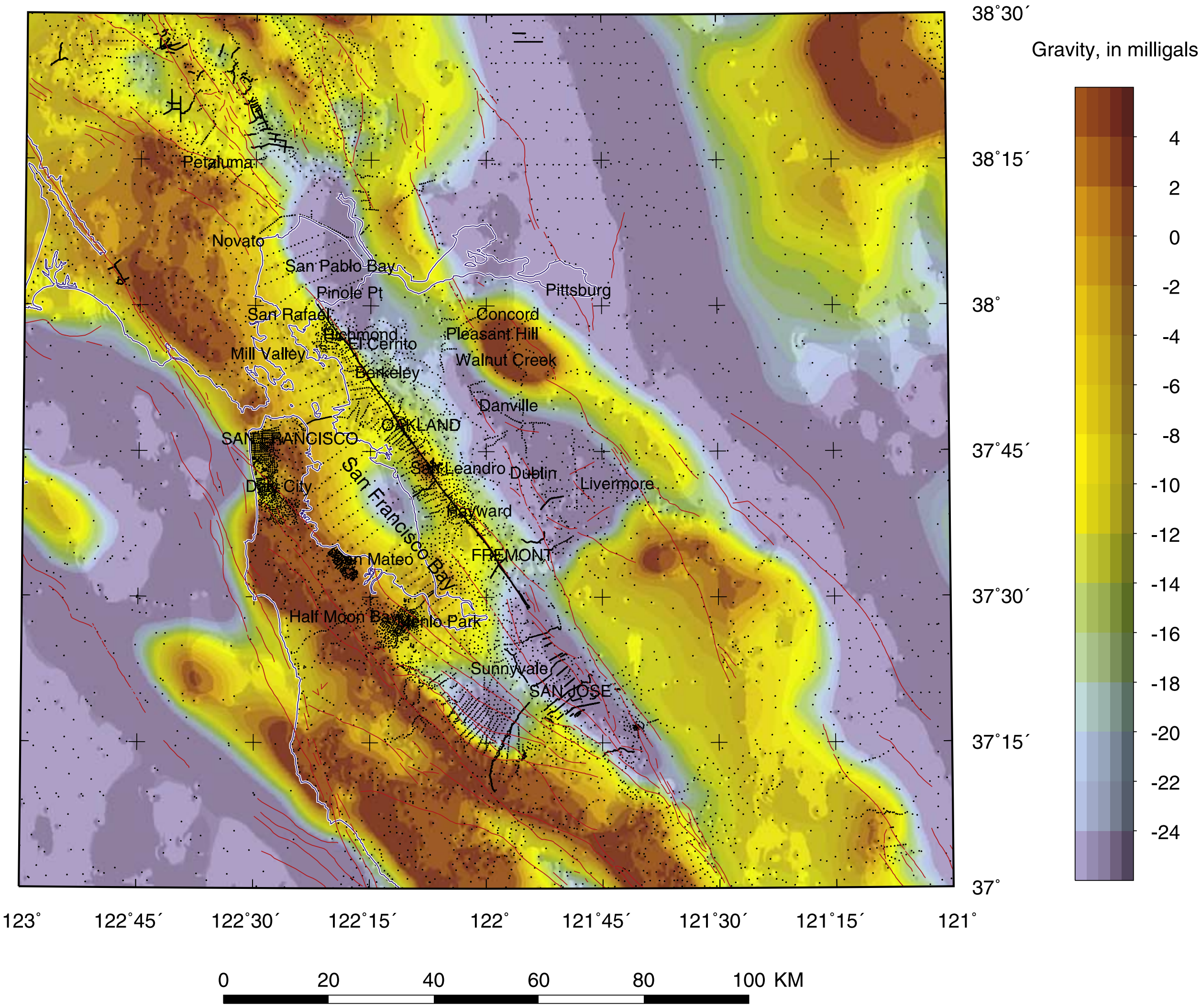

Figure 2. Isostatic gravity map of the Hayward Fault and vicinity. Black triangle, gravity station. Explanation as in Figure 1.

the northeast. All of the ophiolitic rocks and lowest Great Valley Sequence strata crop out within the Hayward Fault Zone itself and probably represent remnants of oceanic crust and pelagic deposits that form a dismembered and discontinuous belt along the entire Hayward Fault. Near Hayward and San Lenadro (Figure 1), a gabbro body, hereafter to referred to as the San Leandro gabbro, is exposed within the Hayward Fault Zone [e.g., *Graymer*, 2000; *Ponce et al.*, 2003a].

2. Gravity, Magnetic, and Seismicity Data

2.1. Gravity Data

[5] Gravity data were collected as part of ongoing studies to determine the tectonic setting and earthquake hazards of the greater San Francisco Bay Area. Gravity data were compiled from previously published [*Snyder et al.*, 1981; *Ponce*, 2001] and recently collected gravity data that result in a high-quality isostatic gravity map (Figure 2). Gravity data were reduced using standard gravity methods and corrections [*Blakely*, 1995], including (1) the earth-tide correction, which corrects for tidal effects of the moon and sun; (2) instrument drift correction, which compensates for drift in the instrument's spring; (3) the latitude correction, which incorporates the variation of the Earth's gravity with latitude; (4) the free-air correction, which accounts for the variation in gravity due to elevation relative to sea level; (5) the Bouguer correction, which corrects for the attraction of material between the station and sea level; (6) the curvature correction, which corrects the

Geochemistry Geophysics Geosystems G3 10.1029/2003GC000684

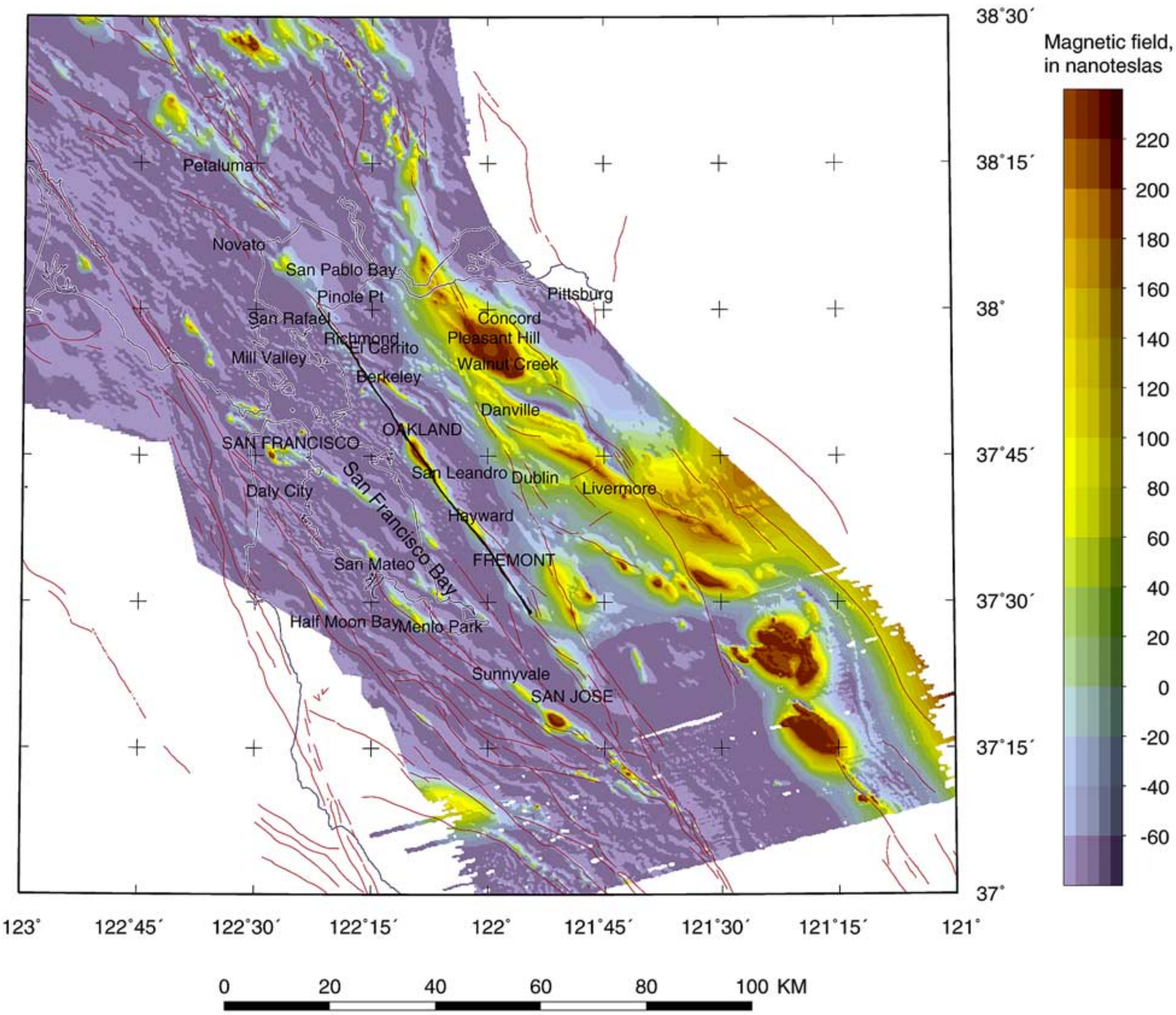

Figure 3. Aeromagnetic map of the Hayward Fault and vicinity. Explanation as in Figure 1.

Bouguer correction for the effect of the Earth's curvature; (7) the terrain correction, which removes the effect of topography to a radial distance of 166.7 km; and (8) the isostatic correction, which removes long-wavelength variations in the gravity field inversely related to topography.

[6] Observed gravity values were referenced to the International Gravity Standardization Net 1971 (IGSN 71) gravity datum [*Morelli*, 1974, p. 18]. Free-air gravity anomalies were calculated using the Geodetic Reference System 1967 formula for theoretical gravity on the ellipsoid [*International Union of Geodesy and Geophysics*, 1971, p. 60] and *Swick*'s [1942, p. 65] formula for the free-air correction. Bouguer, curvature, and terrain corrections were added to the free-air correction to determine the complete Bouguer anomaly at a standard reduction density of 2.67 g/cm^3. Finally, a regional isostatic gravity field (Figure 2) was removed from the Bouguer gravity field assuming an Airy-Heiskanen model for isostatic compensation of topographic loads [*Jachens and Roberts*, 1981] with an assumed nominal or sea level crustal thickness of 25 km, a crustal density of 2.67 g/cm^3, and a density contrast across the base of the model of 0.4 g/cm^3. Gravity values are expressed in milligals (mGal), a unit of acceleration or gravitational force per unit mass equal to 10^{-5} m/s^2.

2.2. Magnetic Data

[7] Two high-resolution aeromagnetic surveys are available within the study area. An aeromagnetic

survey of Livermore and vicinity [*U.S. Geological Survey*, 1992] was flown in a N70°E direction, with a flight-line spacing of 500 m, and a nominal flight-line elevation of 250 m above water and 300 m above land. Data were spaced about 50 m apart along each flightline. The other survey covers the central San Francisco Bay area [*U.S. Geological Survey*, 1996] and was flown in a NE direction with the same flight-line specifications. Aeromagnetic flightline locations and elevations were maintained by precise navigation using a Global Positioning System (GPS). Magnetic data were compiled, leveled along their adjoining boundary, and merged using standard techniques [*Blakely*, 1995] and were corrected for diurnal fluctuations of the Earth's magnetic field. An International Geomagnetic Reference Field (IGRF) of the Earth [*Langel*, 1992], updated to the year of the survey, was also removed from the aeromagnetic data to yield total magnetic field anomalies (Figure 3).

2.3. Seismicity Data

[8] Interpretation of seismicity data obtained from the USGS's Northern California Seismic Network (NCSN) earthquake catalog is hampered by mislocation errors and un-modeled velocity contrasts across the fault. (These data are available from the Northern California Earthquake Data Center: http://quake.geo.berkeley.edu.) To remedy this situation, a regional relocation of hypocenters [*Ellsworth et al.*, 2000] was accomplished using a high-resolution double-difference method [*Waldhauser and Ellsworth*, 2000, 2002] that analyzed and relocated northern California earthquakes from 1984 to 2000, with over 26,000 events within the San Francisco Bay Area (Figure 1). Although the *Waldhauser and Ellsworth* [2002] data set is of higher resolution, a resolution on the order of ten's of meters, the data set contains far fewer events and does not extend much beyond the recent trace of the Hayward Fault (Figure 1).

[9] The double-difference method incorporates ordinary travel time measurements and cross correlation of *P* and *S* wave differential travel time measurements. Residuals between observed and theoretical travel time differences are minimized for pairs of earthquakes. The method essentially minimizes path anomaly bias (location errors) due to un-modeled velocity structure without the use of station corrections. The resulting relative hypocentral errors are about 100 m in epicenter and about 250 m in depth [e.g., *Ellsworth et al.*, 2000]. Absolute location uncertainties were not determined but may be dramatically improved compared to NCSN catalog data. However, a fundamental limitation in differencing algorithms is that for velocity structure that strongly varies with earthquake location, path anomaly bias can only be reduced between closely spaced events [*Wolfe*, 2002]. An analysis of several relocation methods was also discussed by *Wolfe* [2002], and recently, *Zhang and Thurber* [2003] describe a new approach using double-difference seismic tomography that avoids some of the disadvantages of other double-difference methods such as ray path geometry.

3. Discussion

3.1. Gravity

[10] In general, isostatic gravity anomalies (Figure 2) reflect lateral (horizontal) density variations in the middle to upper crust. Thus gravity anomalies can be used to infer the subsurface structure of known or presently unknown geologic features. Gravity anomalies often reflect the distribution of basement rocks, plutonic rocks, calderas, deep sedimentary basins, and linear geologic features such as faults. These geologic features often play an important role in deciphering geologic structure, and their distribution is important in understanding the tectonic and geologic framework of an area.

[11] The Hayward Fault Zone itself is characterized by a steep gravity gradient that reflects a density contrast across the fault between Franciscan Complex rocks on the west and predominantly lower-density Tertiary sedimentary and Great Valley sequence rocks on the east [see *Ponce et al.*, 2003a]. Along the Hayward fault, a prominent gravity low west of San Leandro indicates the presence of an offshore sedimentary basin about 1.5 km thick [*Marlow et al.*, 1999]. An isostatic gravity high east of the city of San Leandro reflects a high density gabbroic body, the San Leandro gabbro, with an average saturated bulk density of 2.88 g/cm^3.

3.2. Magnetics

[12] Geologic features often produce low amplitude magnetic fields that perturb the main field

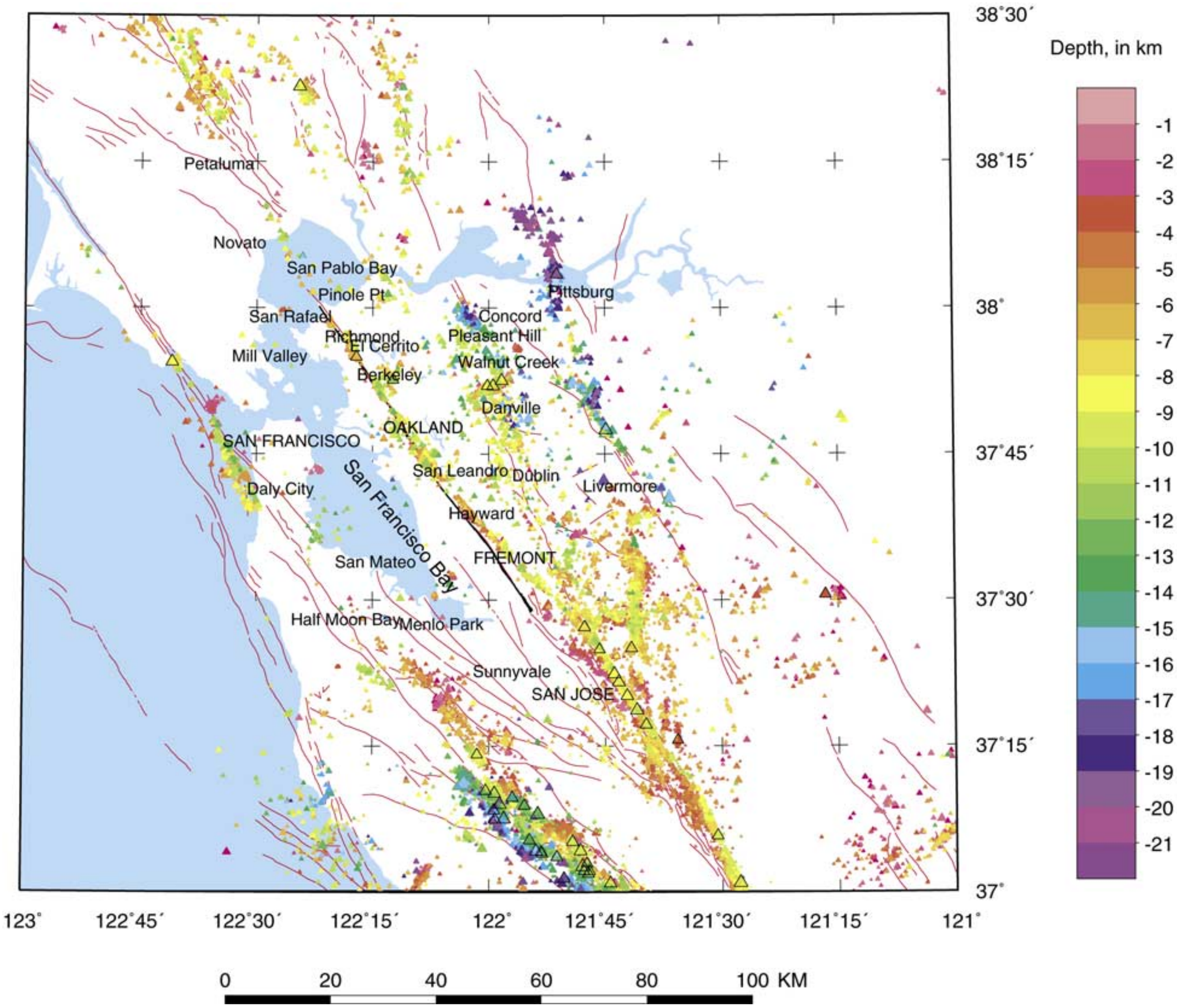

Figure 4. Regional relocated double-difference seismicity map of the Hayward Fault and vicinity. Triangle, relocated seismicity; symbol size is proportional to earthquake magnitude, and colors indicate focal depth. Black triangle, earthquakes $\geq M4$. Explanation as in Figure 1.

of the Earth and can be enhanced by the standard practice of removal of a regional magnetic field. The resulting magnetic anomalies reflect lateral changes in rock magnetic properties and can be analyzed to gain insights into the subsurface structure of the Earth. In general, aeromagnetic anomalies along the Hayward Fault (Figure 3) reflect mafic and ultramafic rocks, volcanic rocks, magnetic sedimentary rocks, and linear geologic features such as faults that juxtapose rocks with contrasting magnetic properties. These features play an important role in deciphering the geologic history and framework of the area. The most prominent magnetic anomaly along the Hayward Fault correlates with a San Leandro gabbro the interpretation of which, combined with geologic and gravity data, has implications for the three-dimensional geometry and evolution of the entire Hayward Fault Zone [*Ponce et al.*, 2003a].

[13] Combined, gravity and magnetic data suggest that the central part of the Hayward Fault Zone dips about 75°NE and independently supports the results of the relocated double-difference seismicity data, and has preferentially followed a preexisting structure delimited in part by the San Leandro gabbro. In addition, the San Leandro gabbro body may influence seismicity along the Hayward Fault, may concentrate or localize stress along the periphery of the body

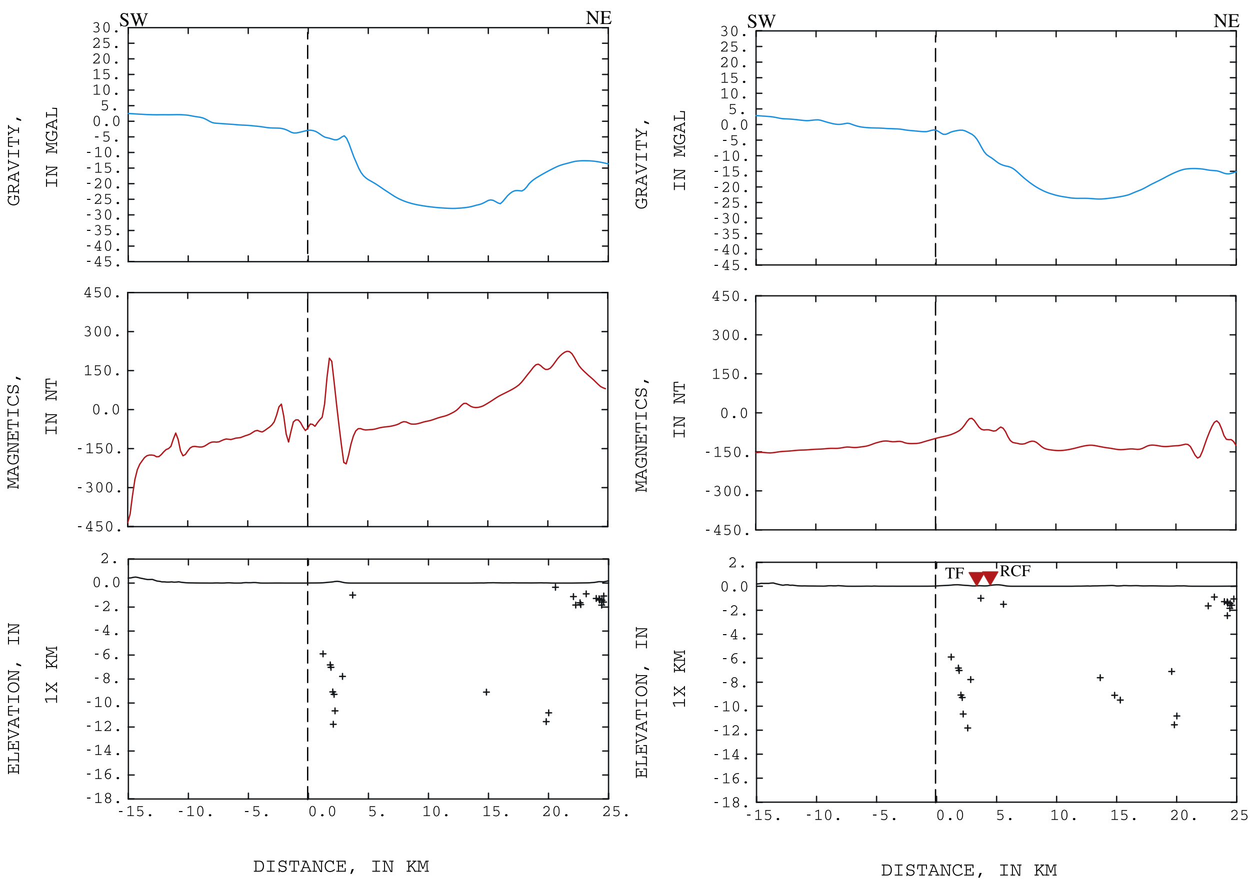

Profile at 17.5 km **Profile at 20.0 km**

Figure A1. Gravity, magnetic, and seismicity data across the Hayward Fault.

Geochemistry Geophysics Geosystems G3 10.1029/2003GC000684

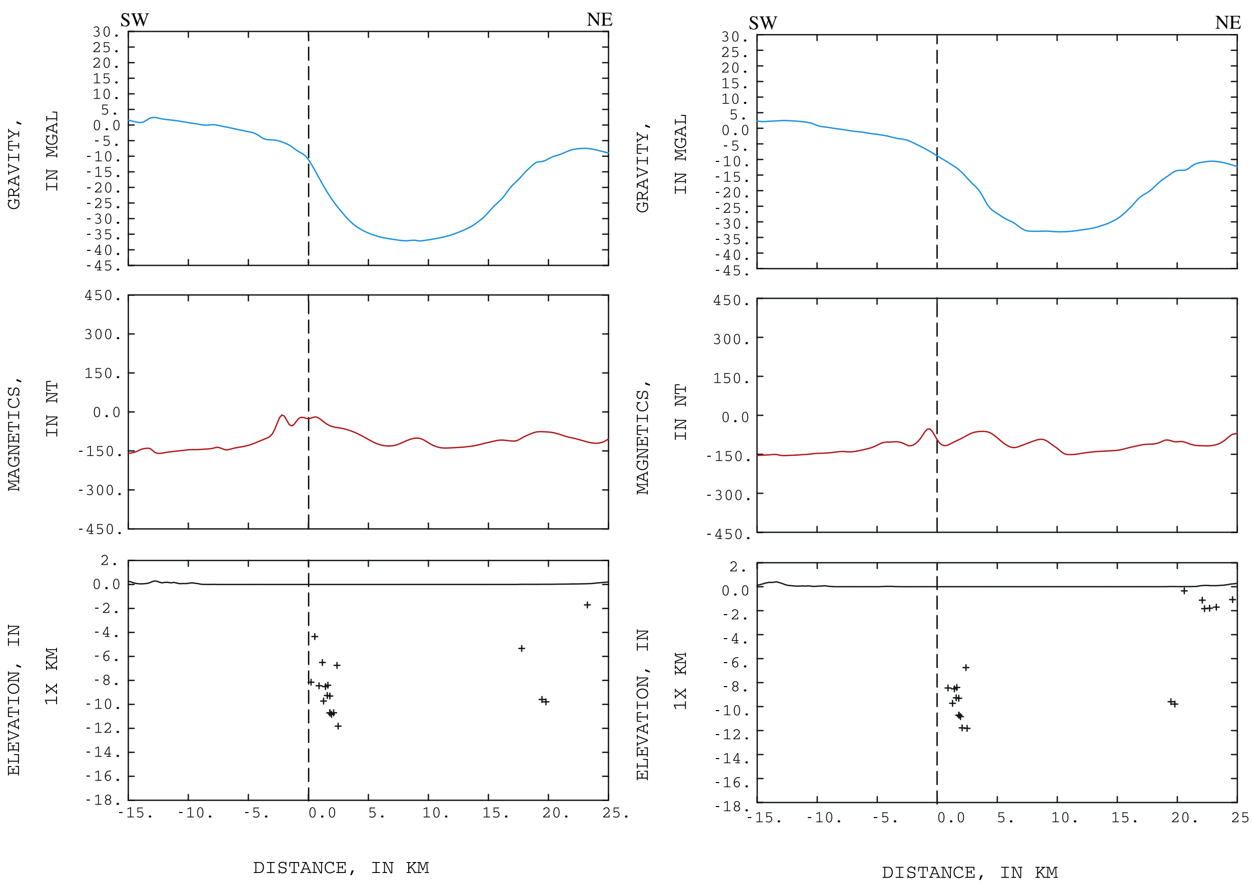

Profile at 12.5 km **Profile at 15.0 km**

Figure A2. Gravity, magnetic, and seismicity data across the Hayward Fault.

10.1029/2003GC000684

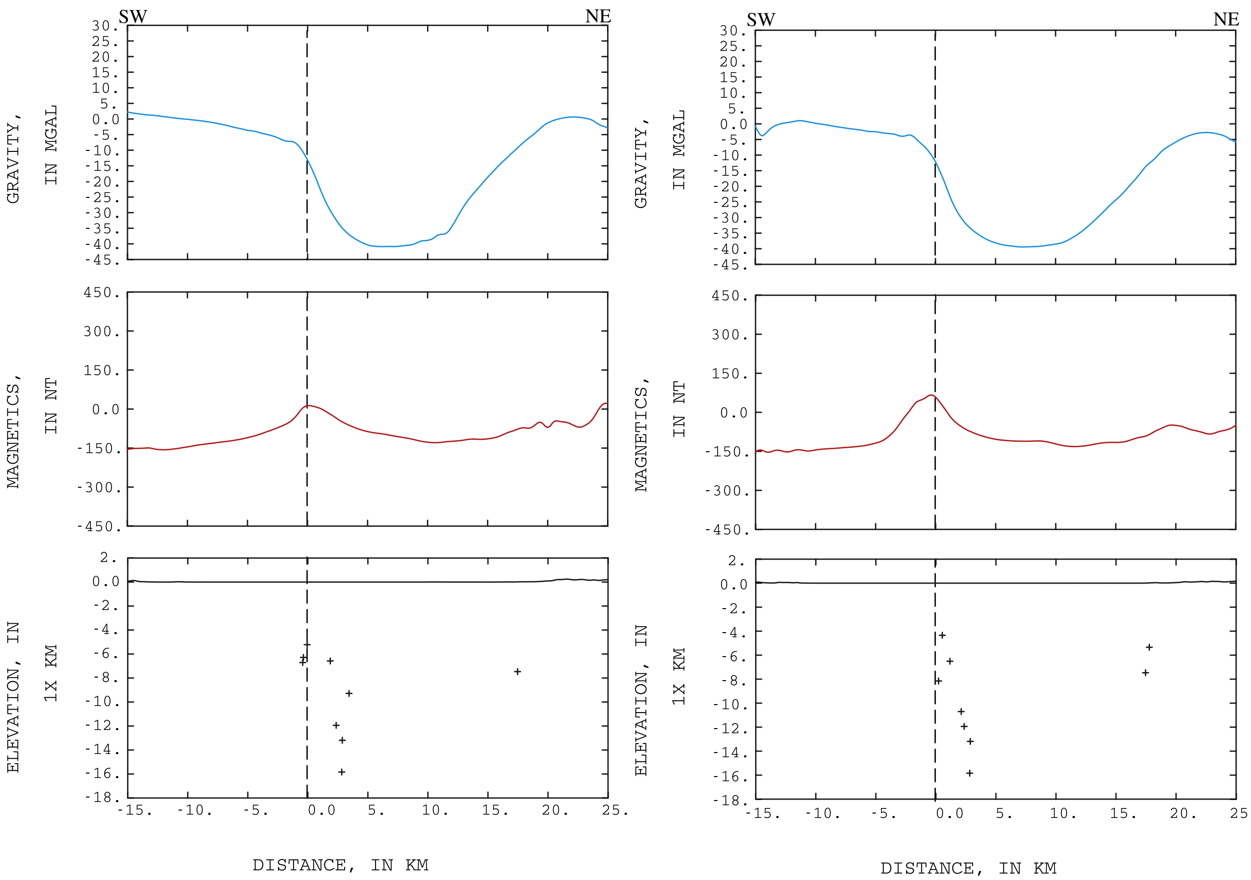

Profile at 7.5 km **Profile at 10.0 km**

Figure A3. Gravity, magnetic, and seismicity data across the Hayward Fault.

10.1029/2003GC000684

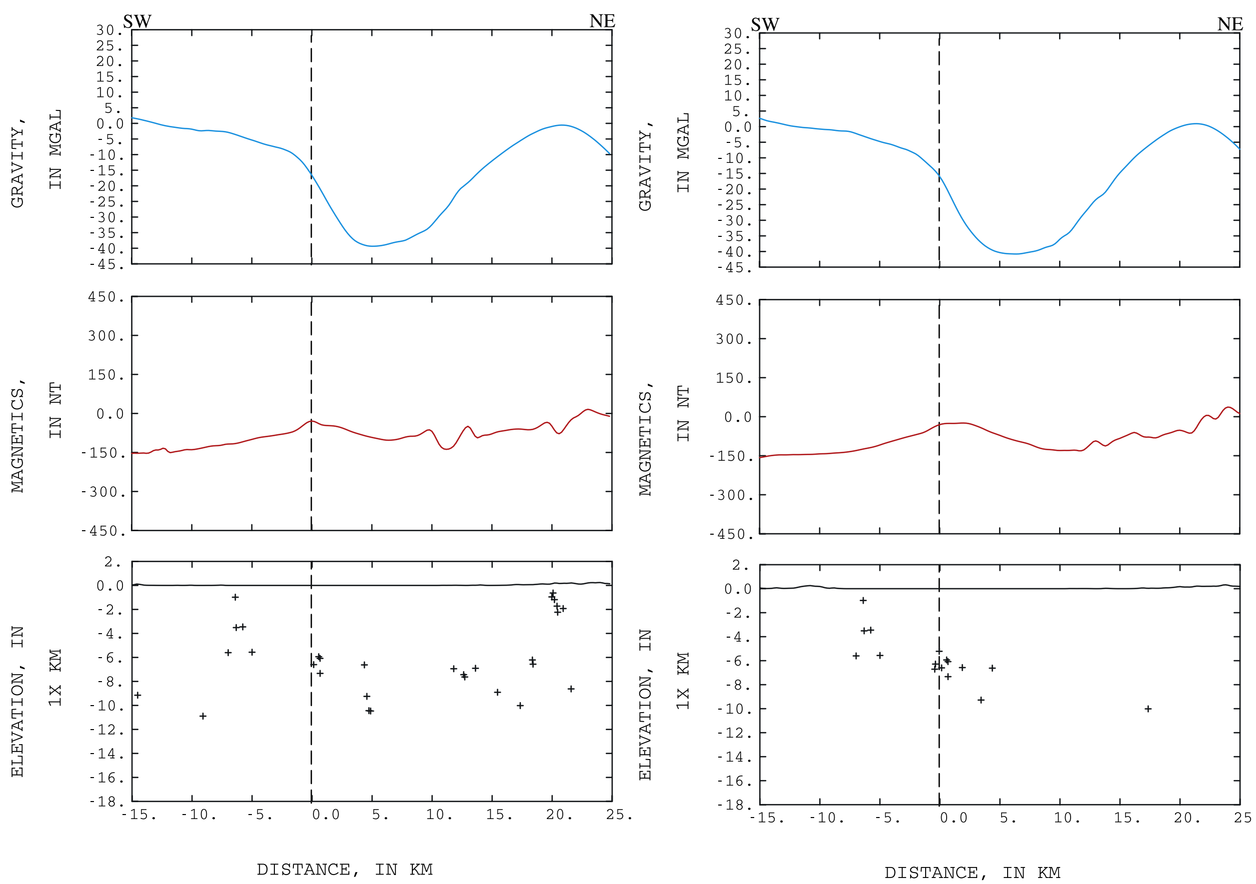

Profile at 2.5 km **Profile at 5.0 km**

Figure A4. Gravity, magnetic, and seismicity data across the Hayward Fault.

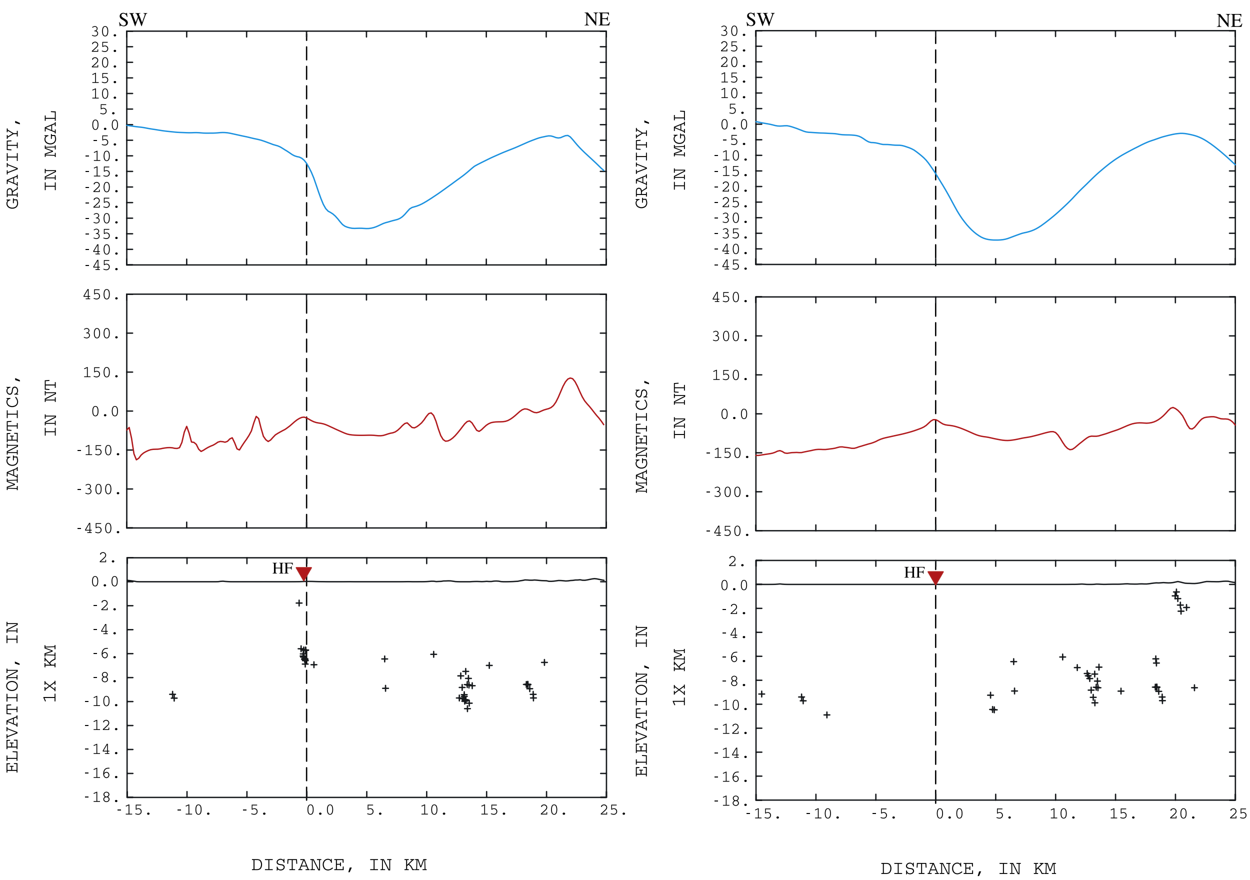

Profile at -2.5 km

Profile at 0.0 km = Pinole Point

Figure A5. Gravity, magnetic, and seismicity data across the Hayward Fault.

10.1029/2003GC000684

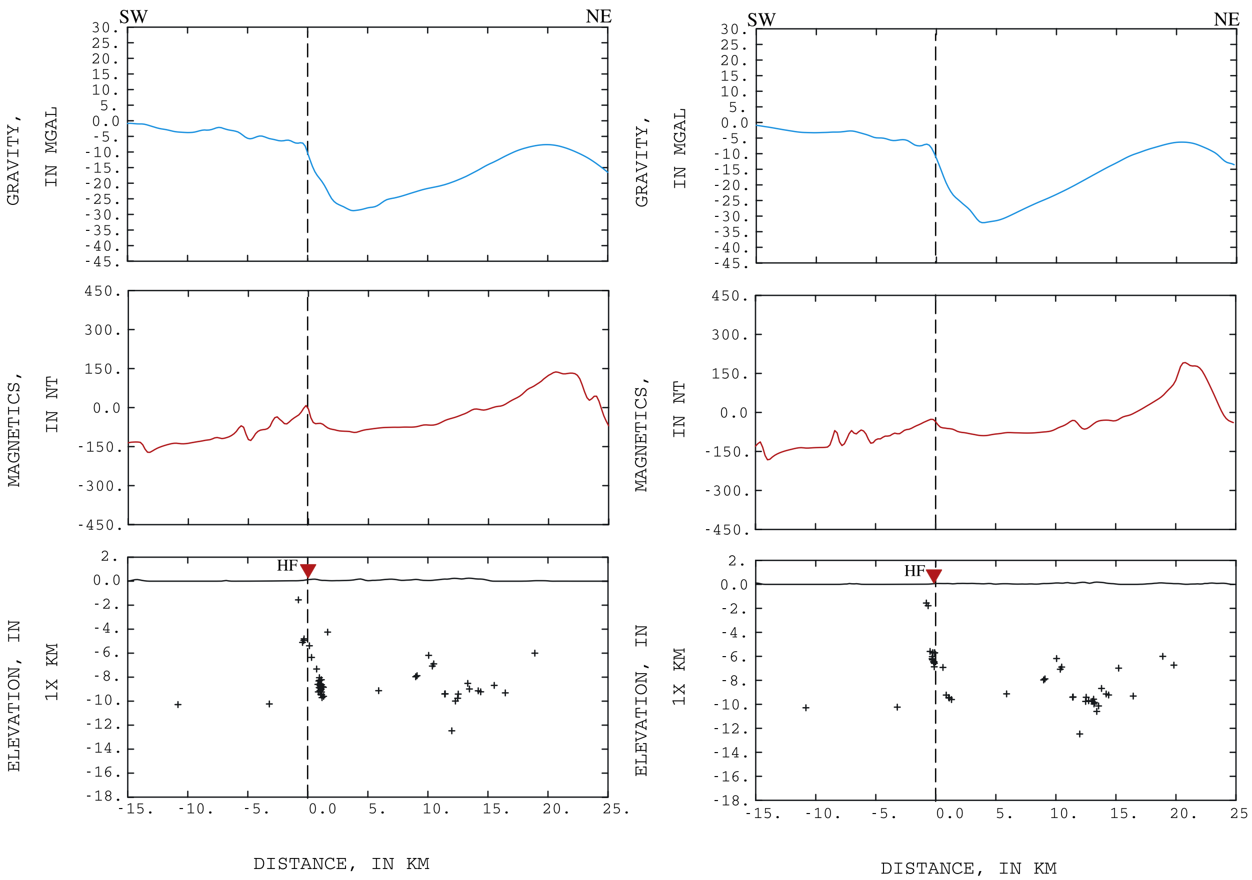

Profile at -7.5 km **Profile at -5.0 km**

Figure A6. Gravity, magnetic, and seismicity data across the Hayward Fault.

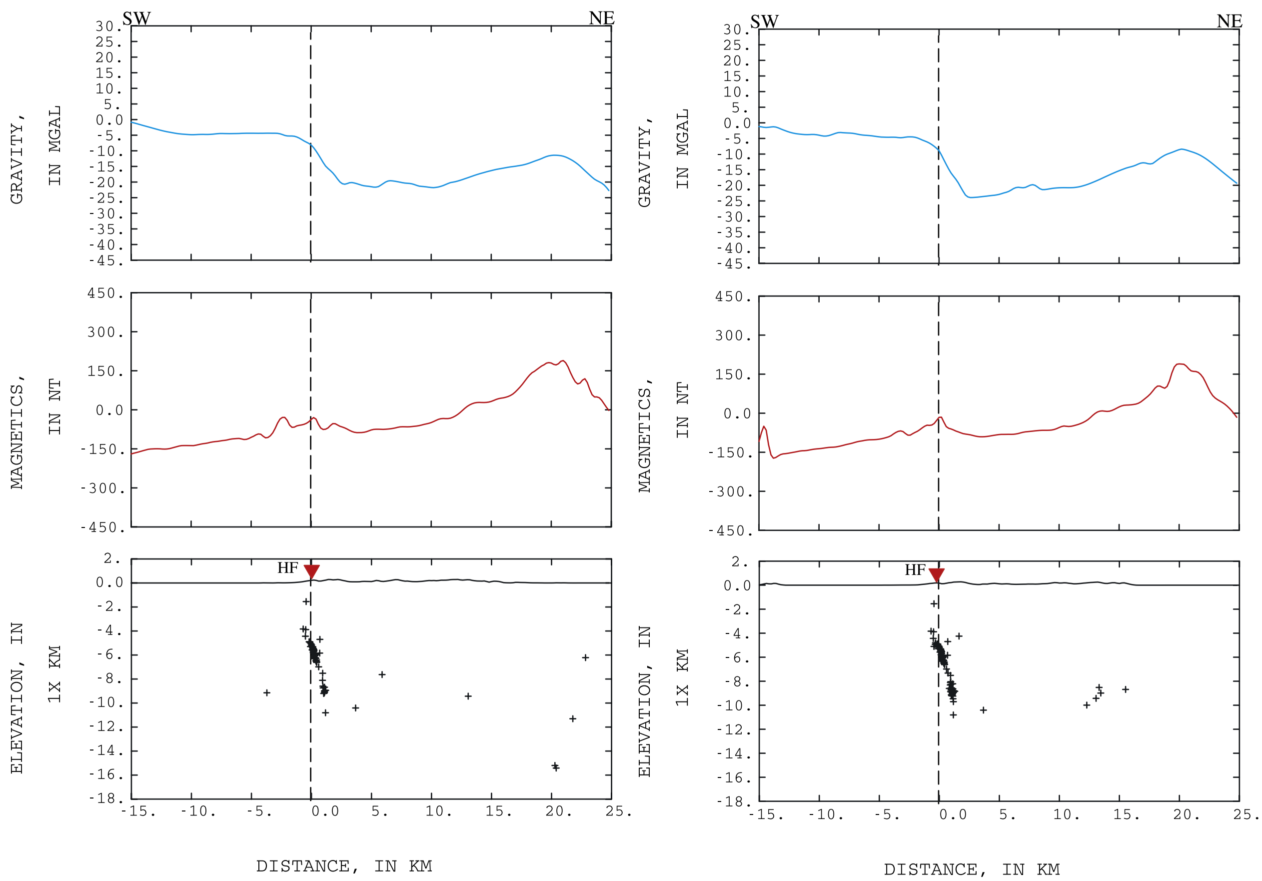

Profile at -12.5 km

Profile at -10.0 km

Figure A7. Gravity, magnetic, and seismicity data across the Hayward Fault.

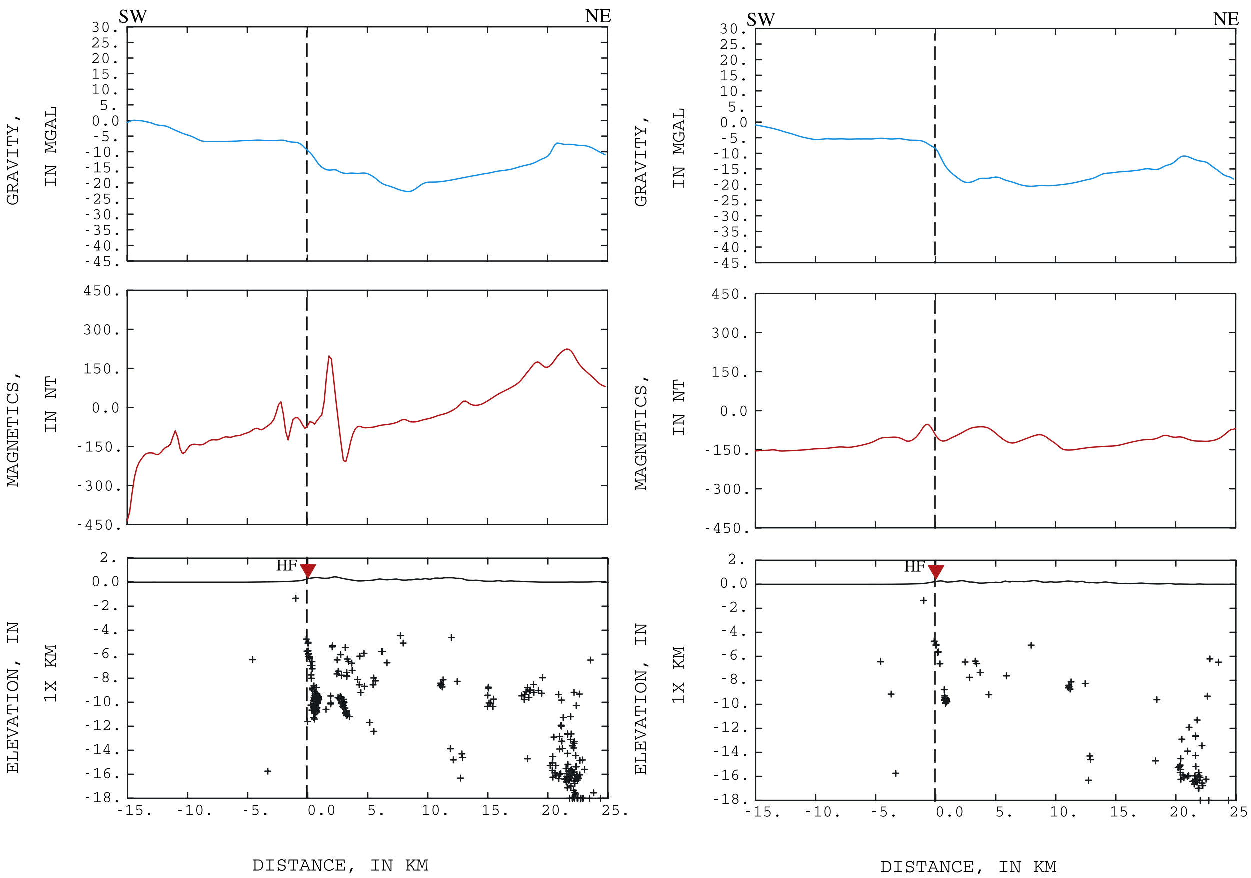

Profile at -17.5 km **Profile at -15.0 km**

Figure A8. Gravity, magnetic, and seismicity data across the Hayward Fault.

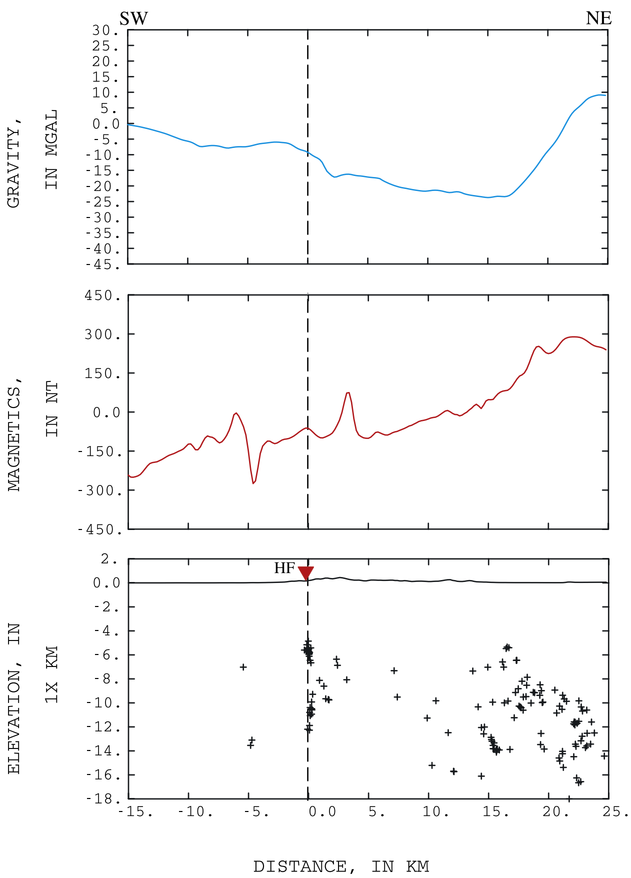

Profile at -22.5 km

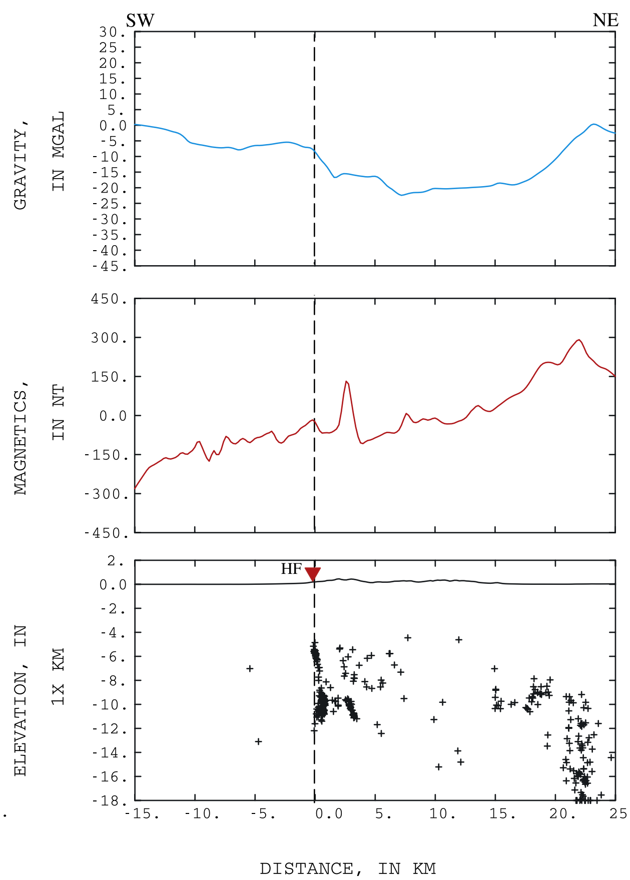

Profile at -20.0 km

Figure A9. Gravity, magnetic, and seismicity data across the Hayward Fault.

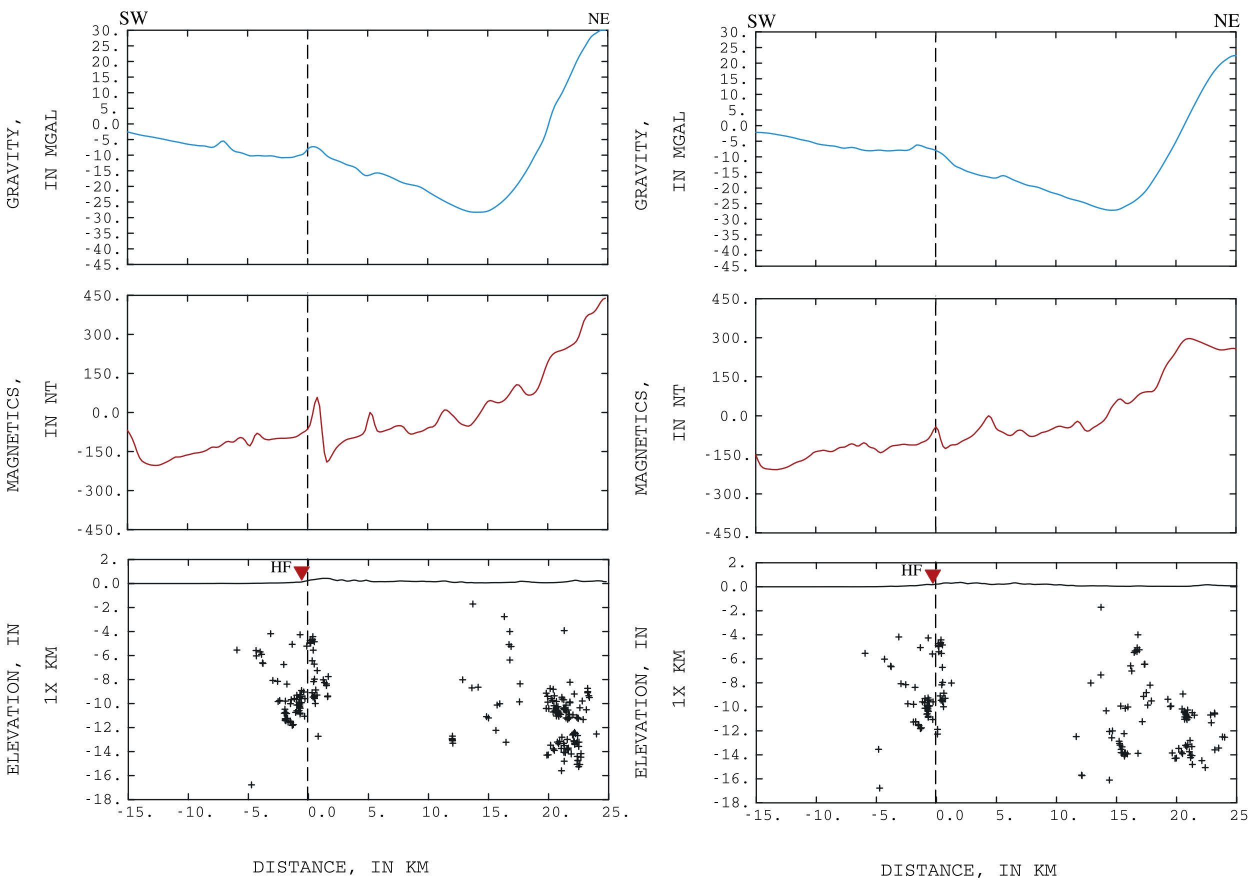

Profile at -27.5 km **Profile at -25.0 km**

Figure A10. Gravity, magnetic, and seismicity data across the Hayward Fault.

10.1029/2003GC000684

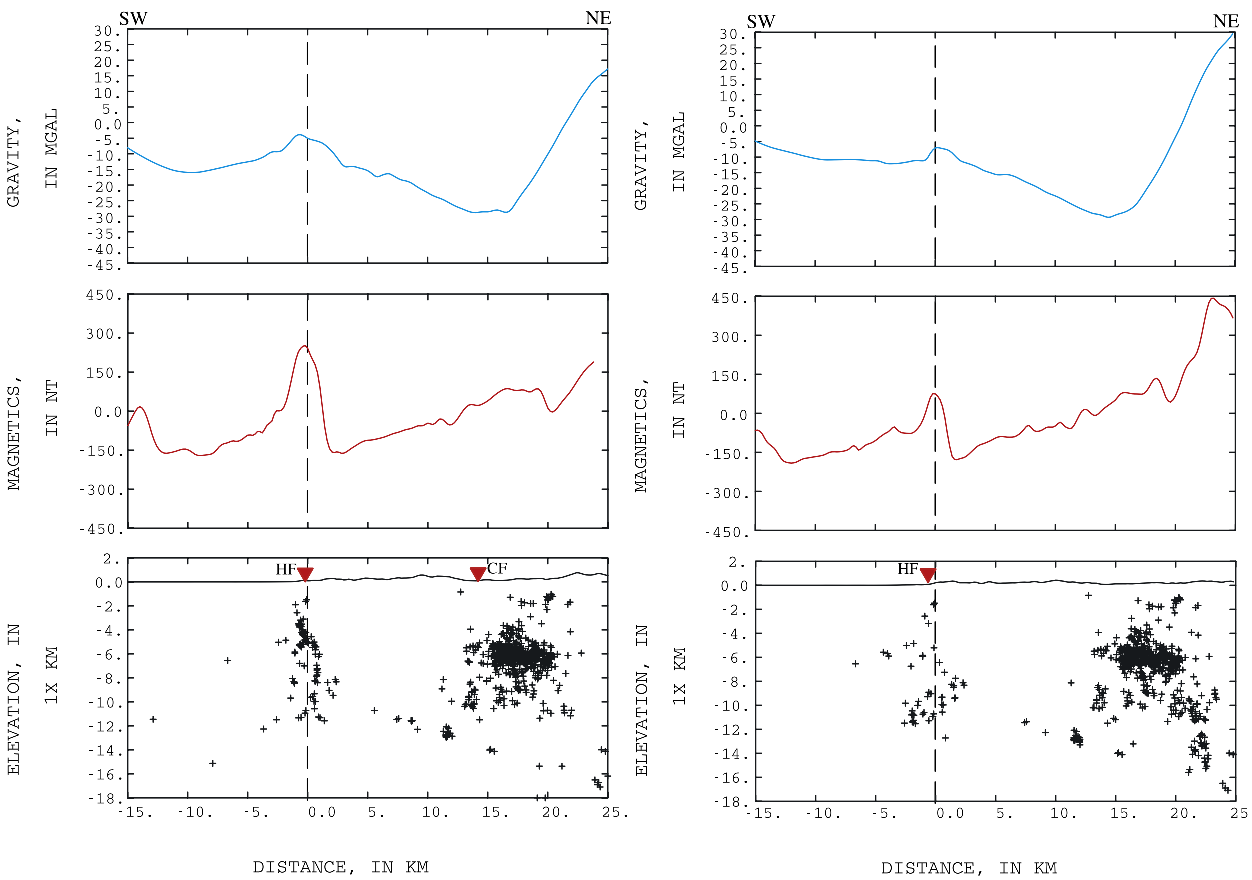

Profile at -32.5 km **Profile at -30.0 km**

Figure A11. Gravity, magnetic, and seismicity data across the Hayward Fault.

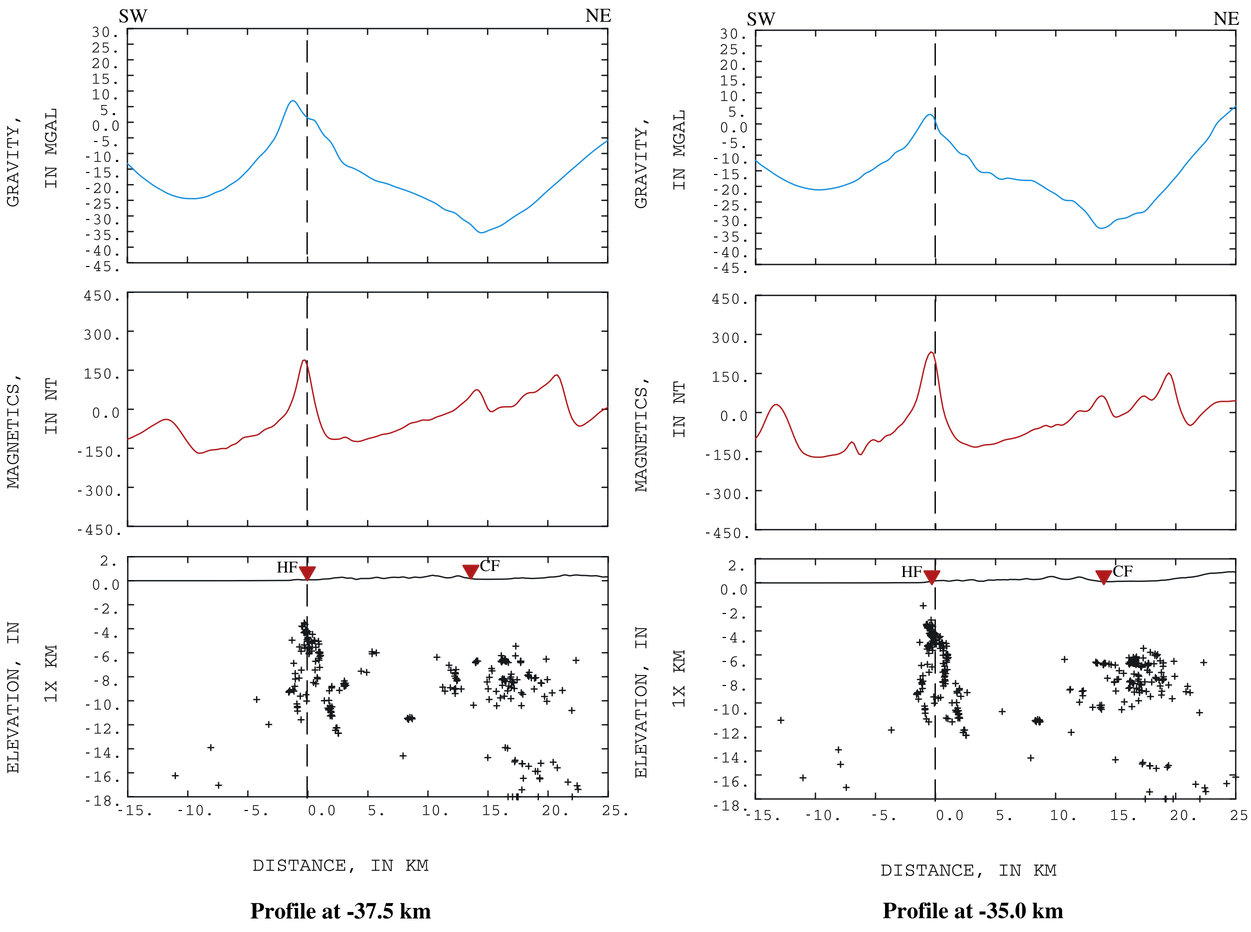

Figure A12. Gravity, magnetic, and seismicity data across the Hayward Fault.

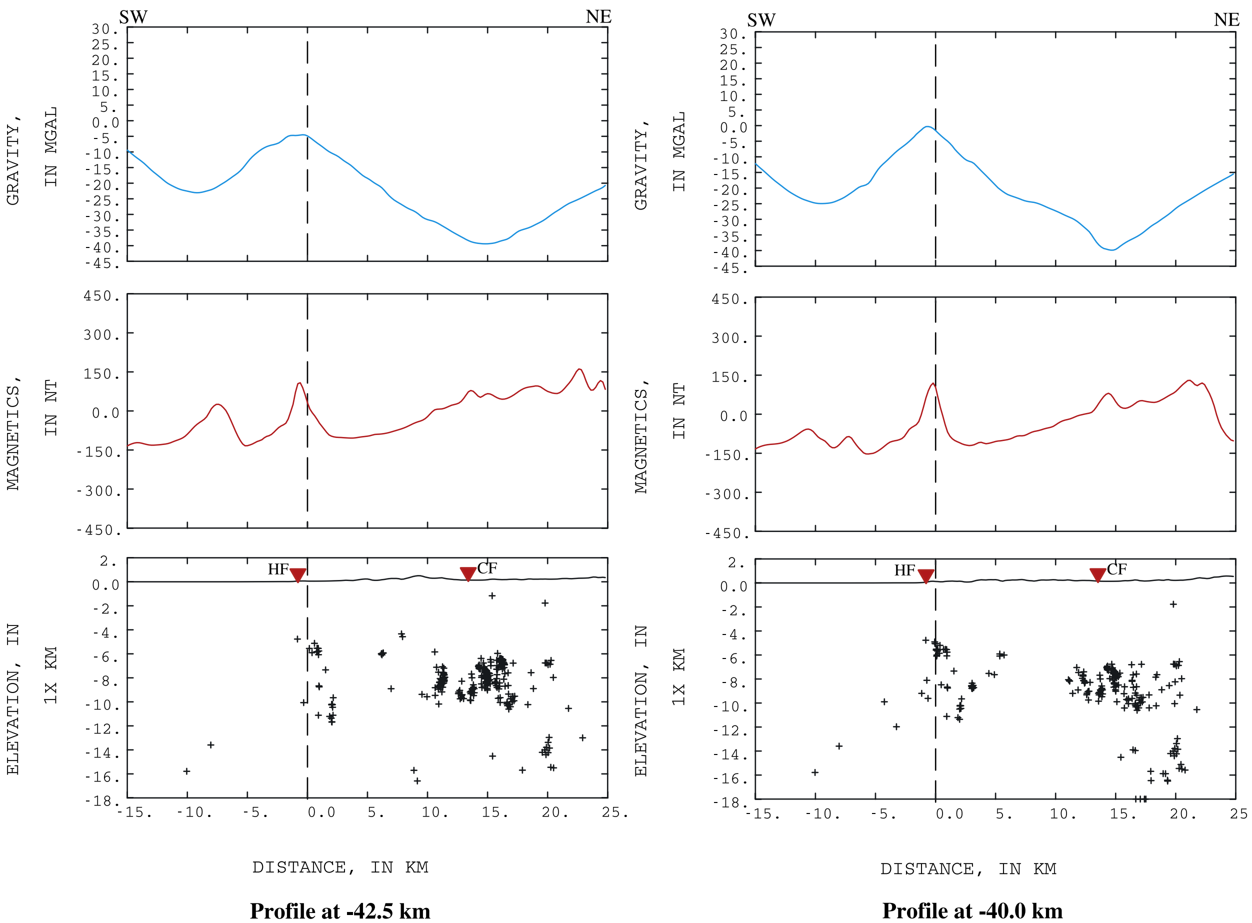

Figure A13. Gravity, magnetic, and seismicity data across the Hayward Fault.

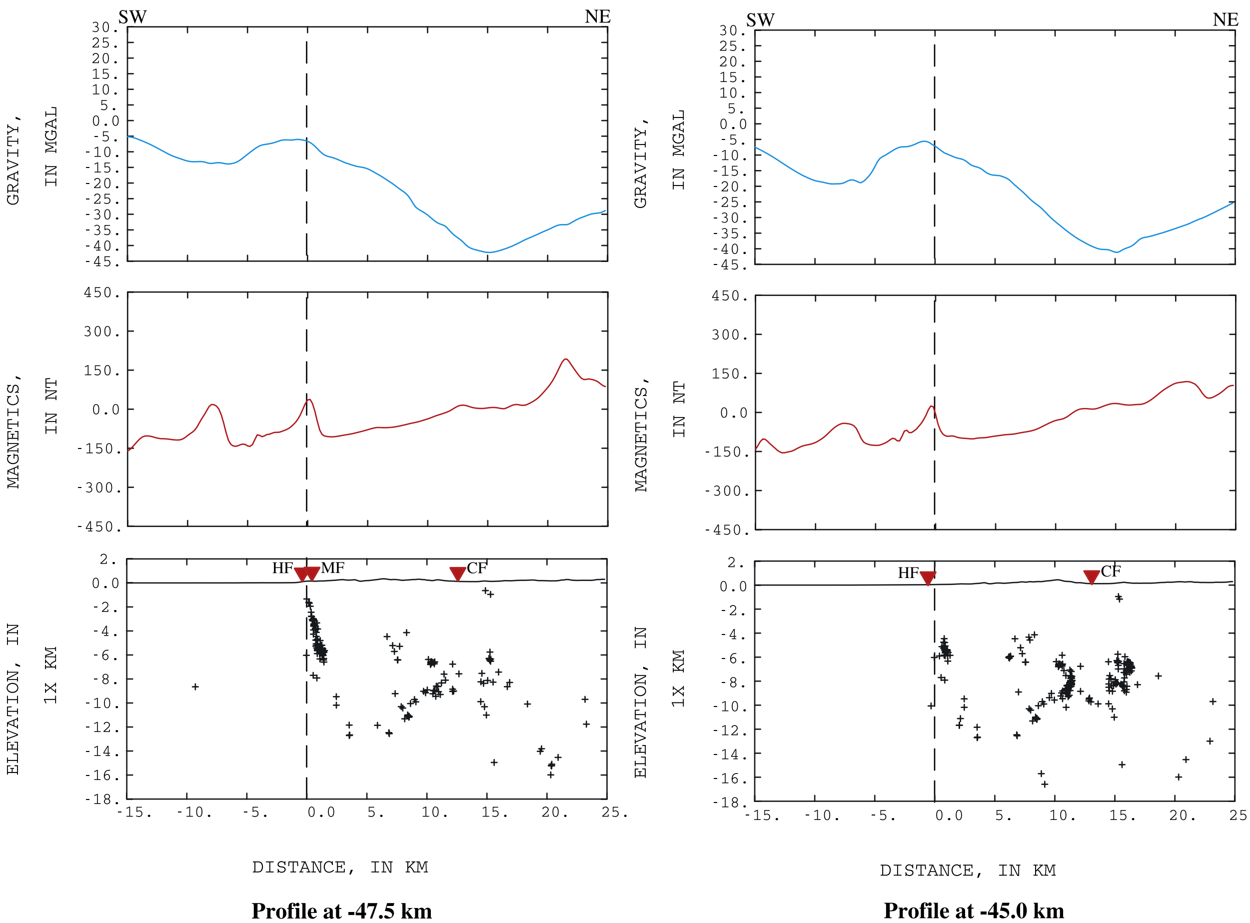

Figure A14. Gravity, magnetic, and seismicity data across the Hayward Fault.

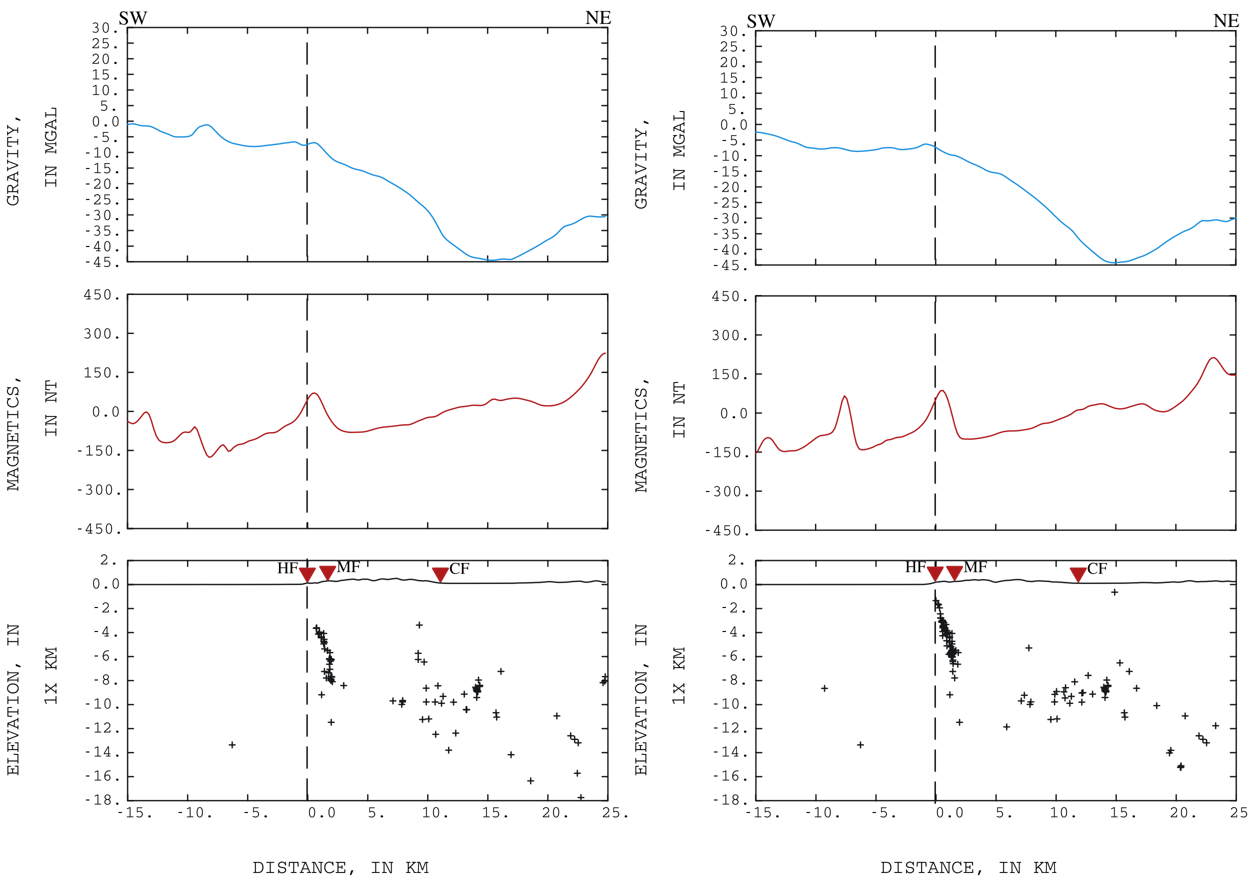

Profile at -52.5 km **Profile at -50.0 km**

Figure A15. Gravity, magnetic, and seismicity data across the Hayward Fault.

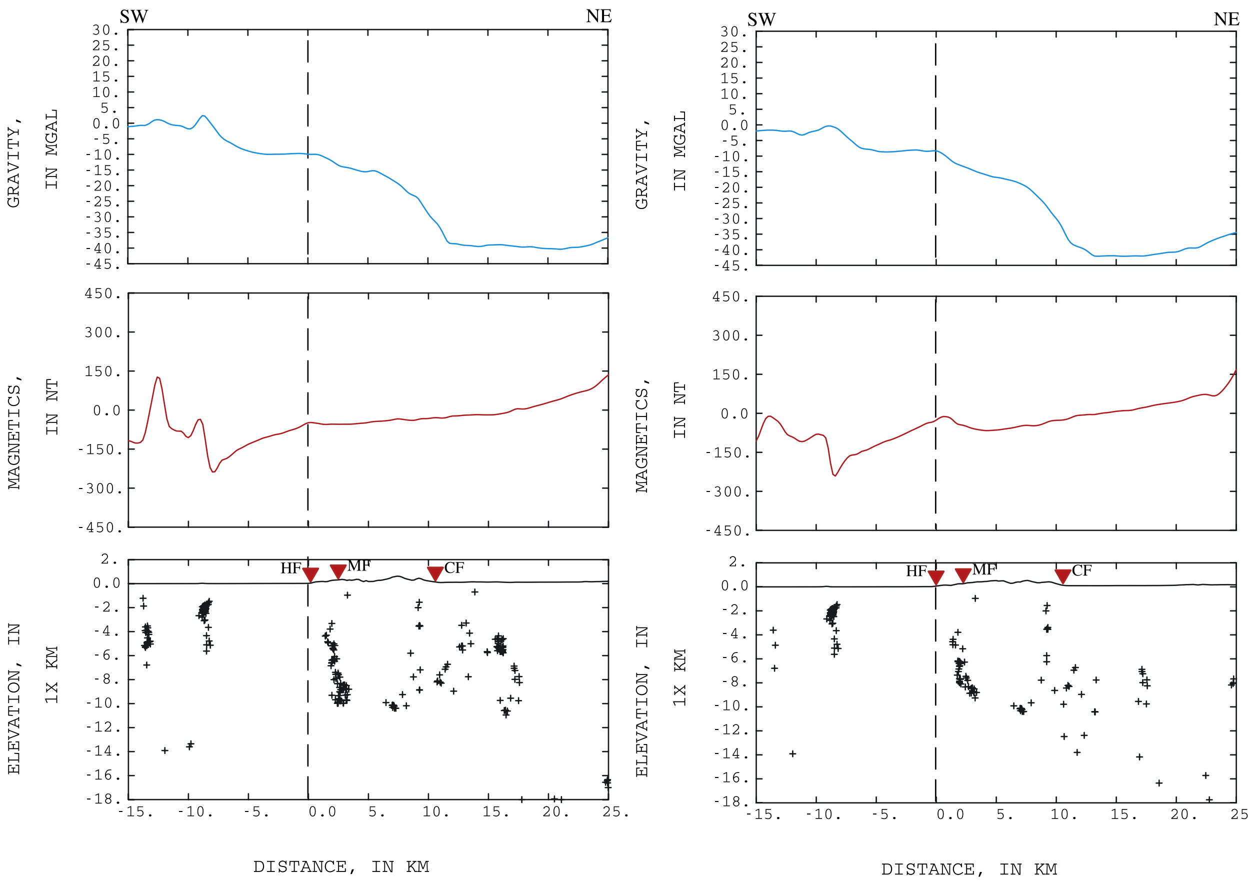

Figure A16. Gravity, magnetic, and seismicity data across the Hayward Fault.

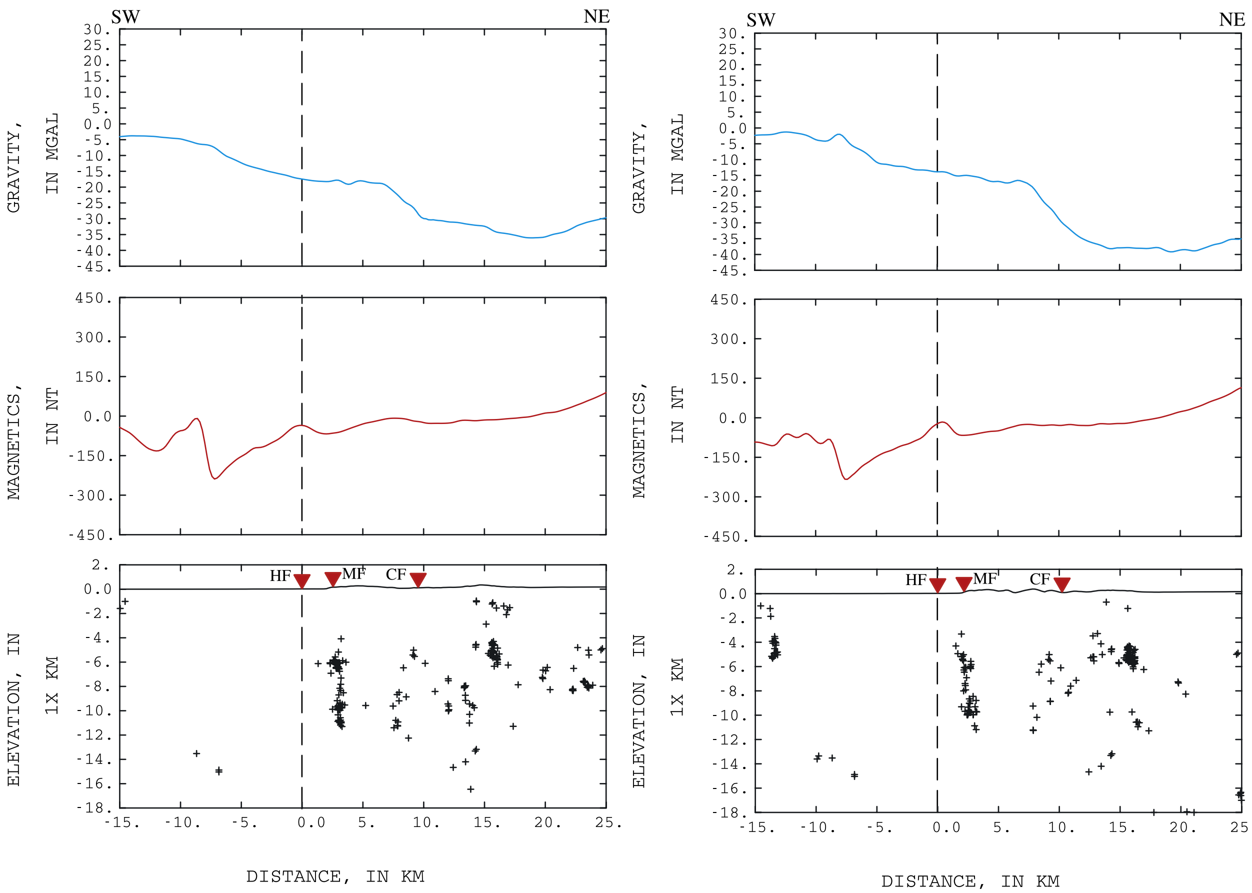

Profile at -62.5 km **Profile at -60.0 km**

Figure A17. Gravity, magnetic, and seismicity data across the Hayward Fault.

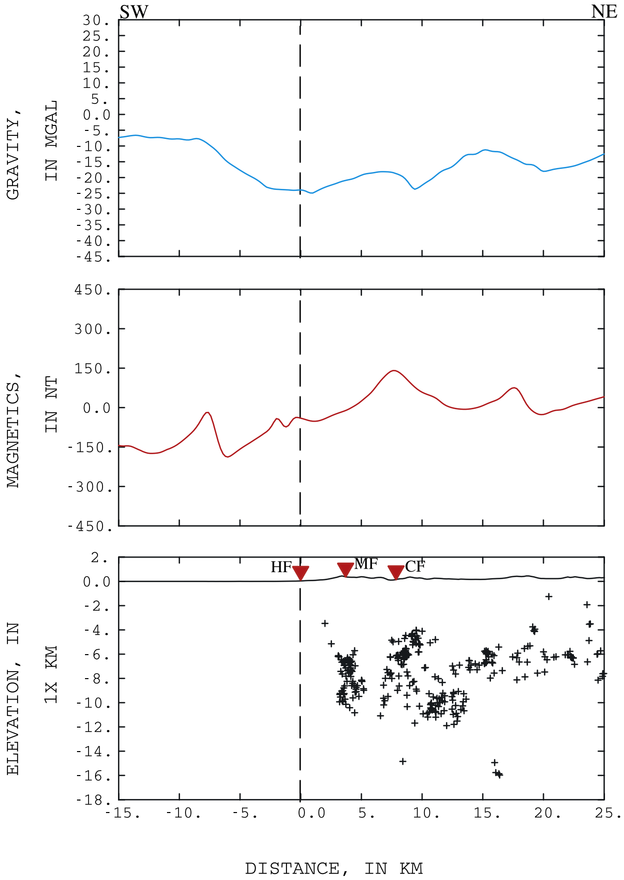

Profile at -67.5 km

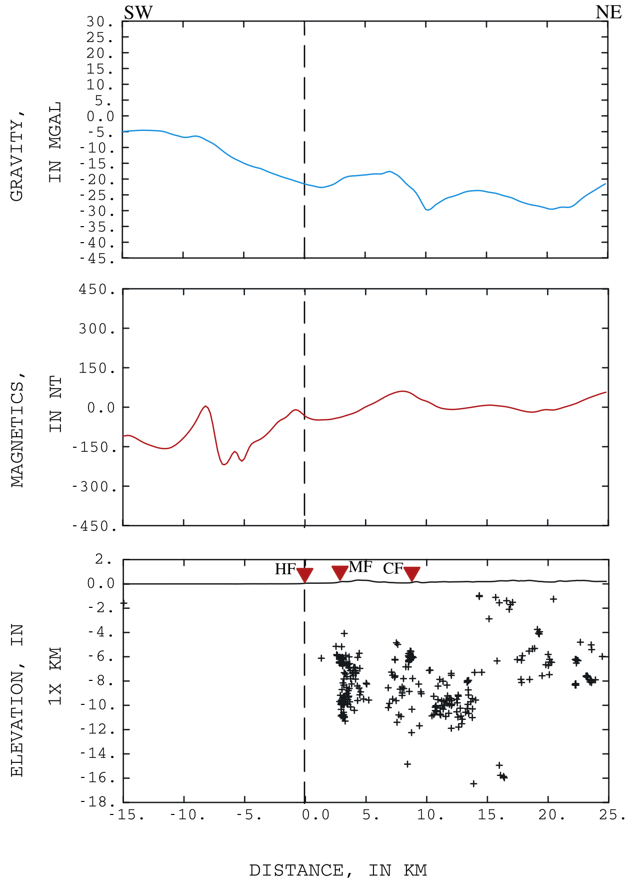

Profile at -65.0 km

Figure A18. Gravity, magnetic, and seismicity data across the Hayward Fault.

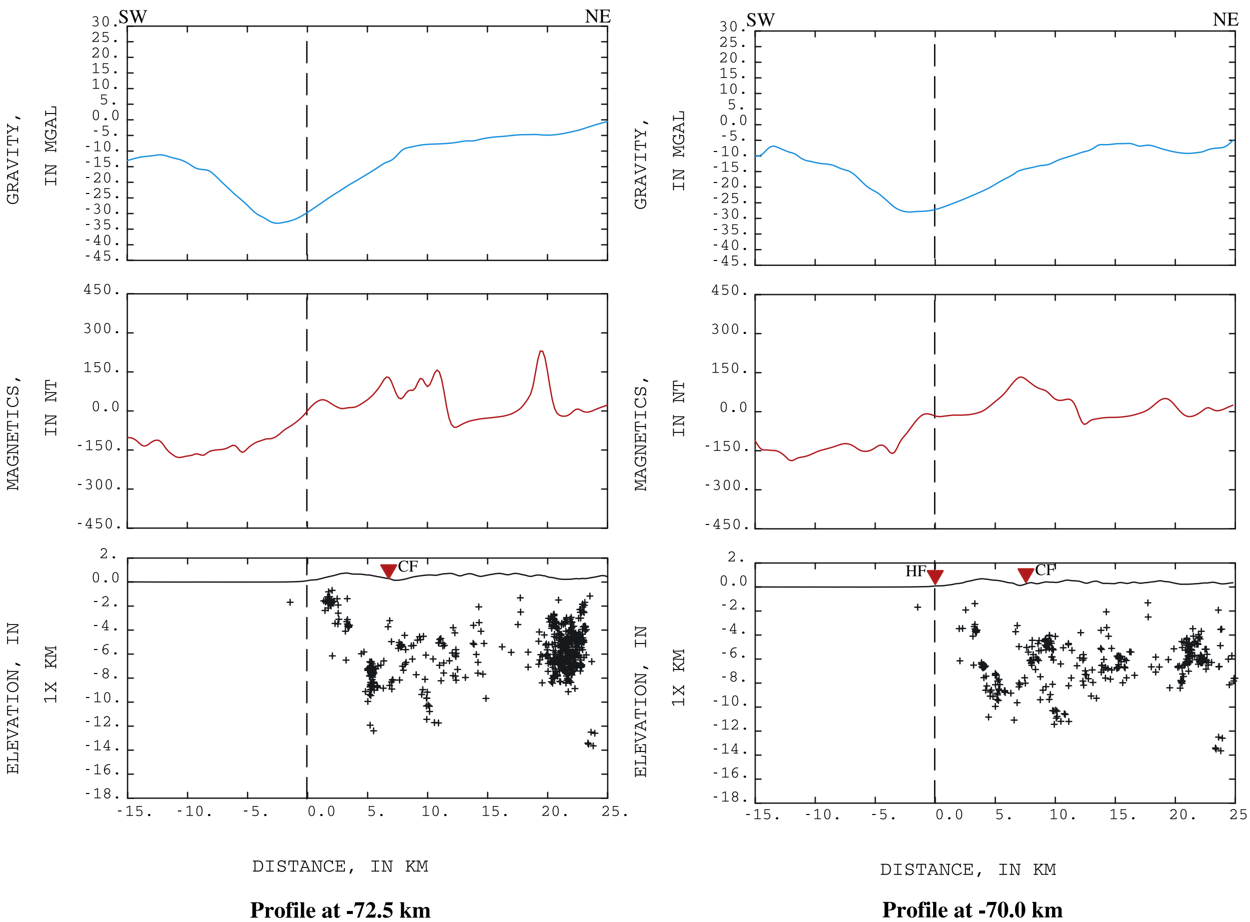

Figure A19. Gravity, magnetic, and seismicity data across the Hayward Fault.

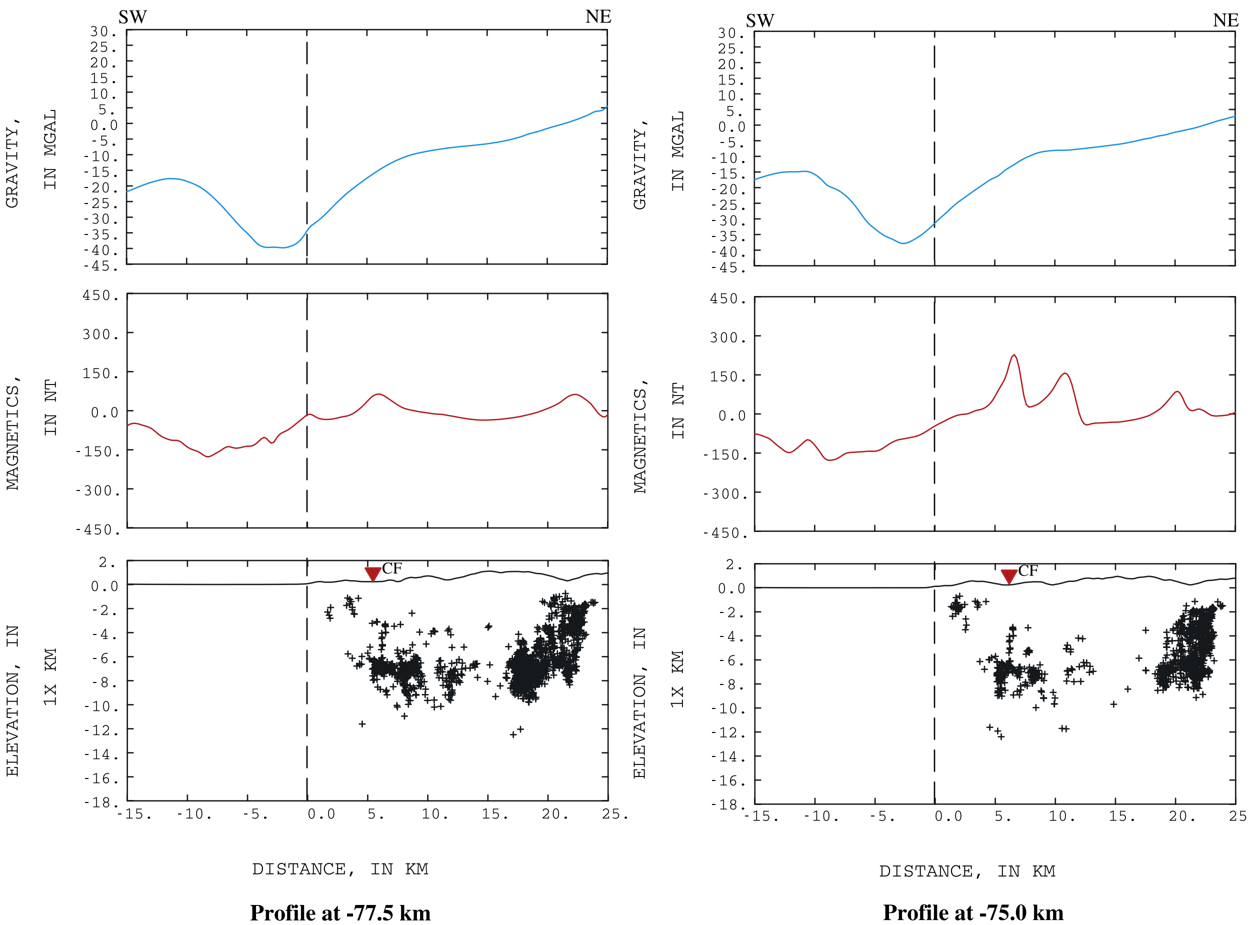

Figure A20. Gravity, magnetic, and seismicity data across the Hayward Fault.

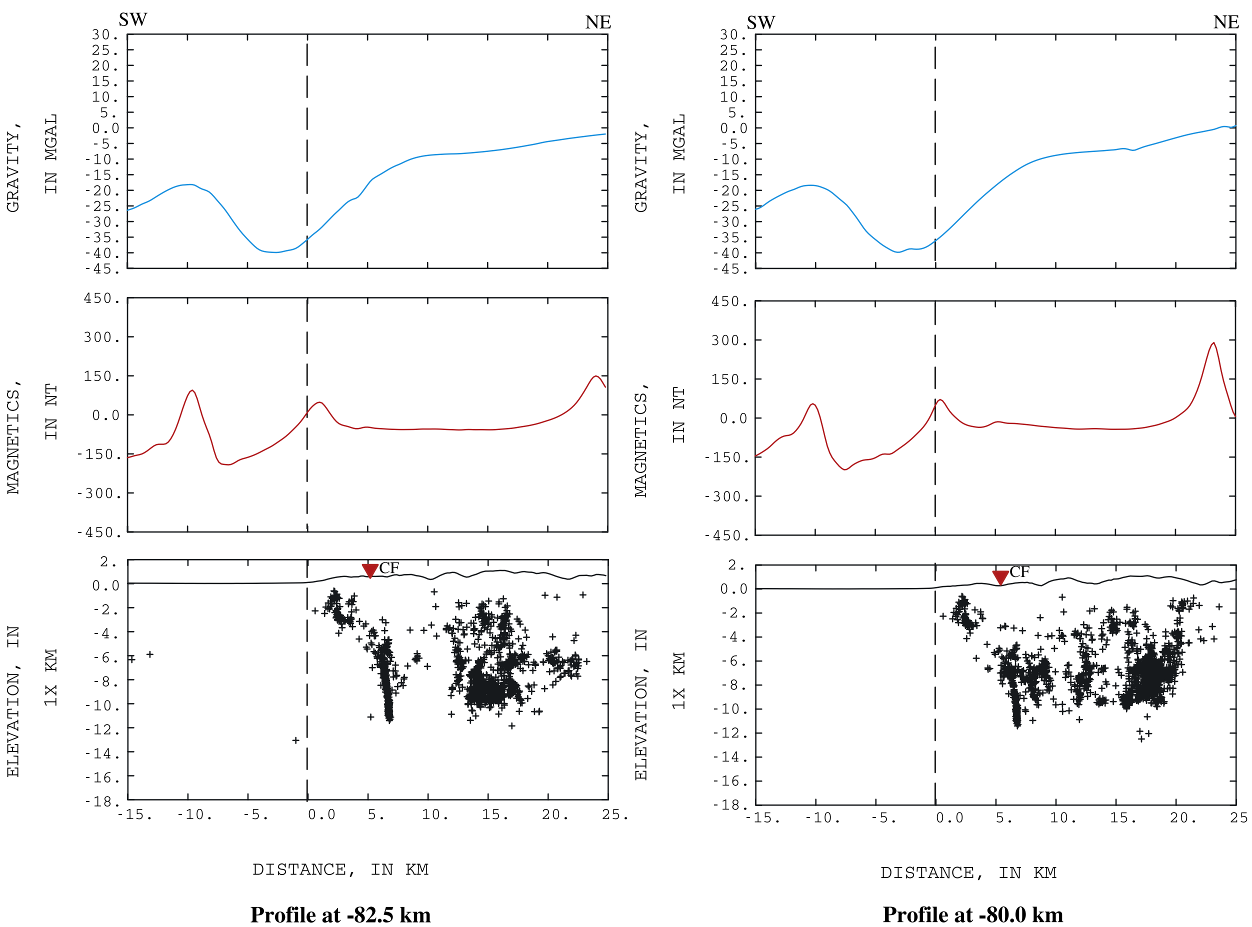

Figure A21. Gravity, magnetic, and seismicity data across the Hayward Fault.

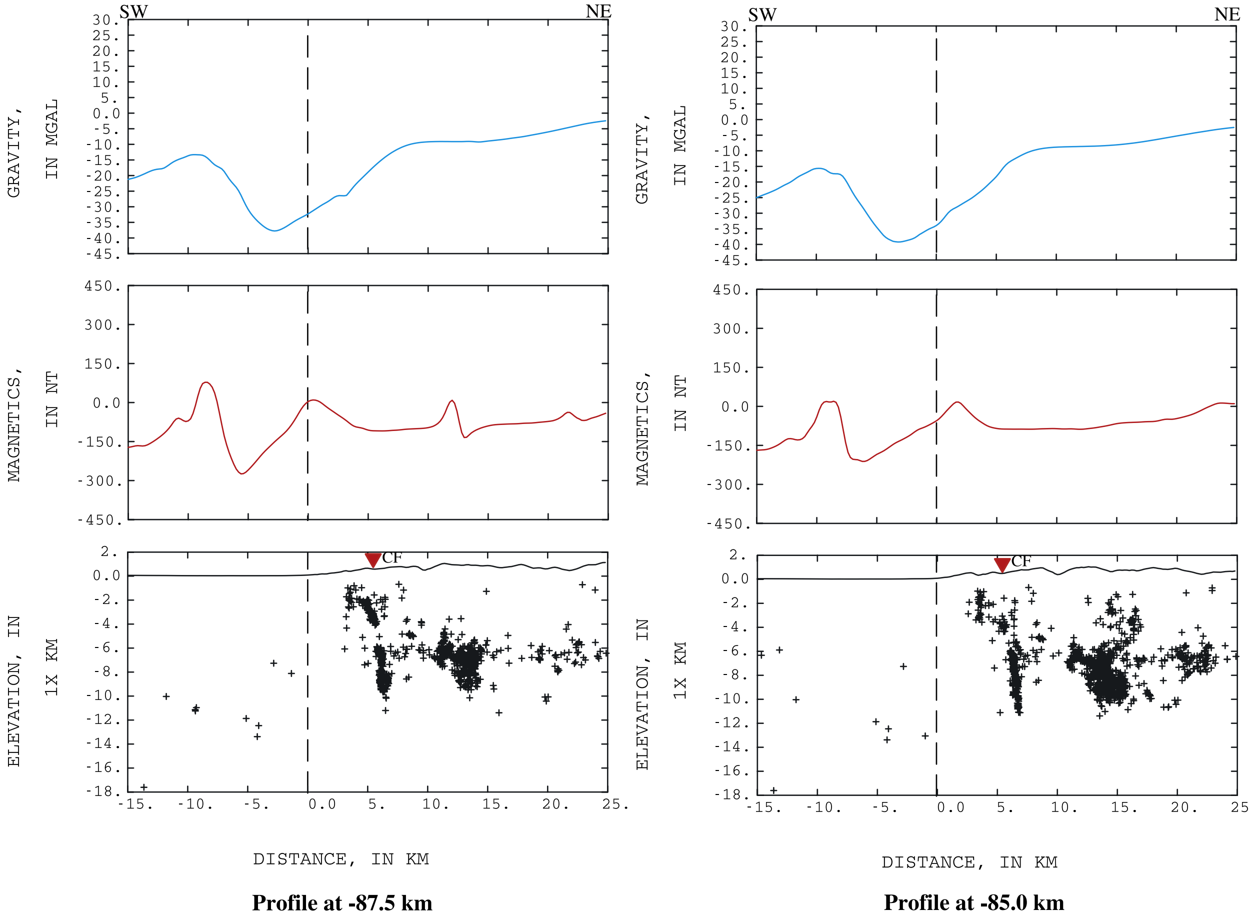

Figure A22. Gravity, magnetic, and seismicity data across the Hayward Fault.

10.1029/2003GC000684

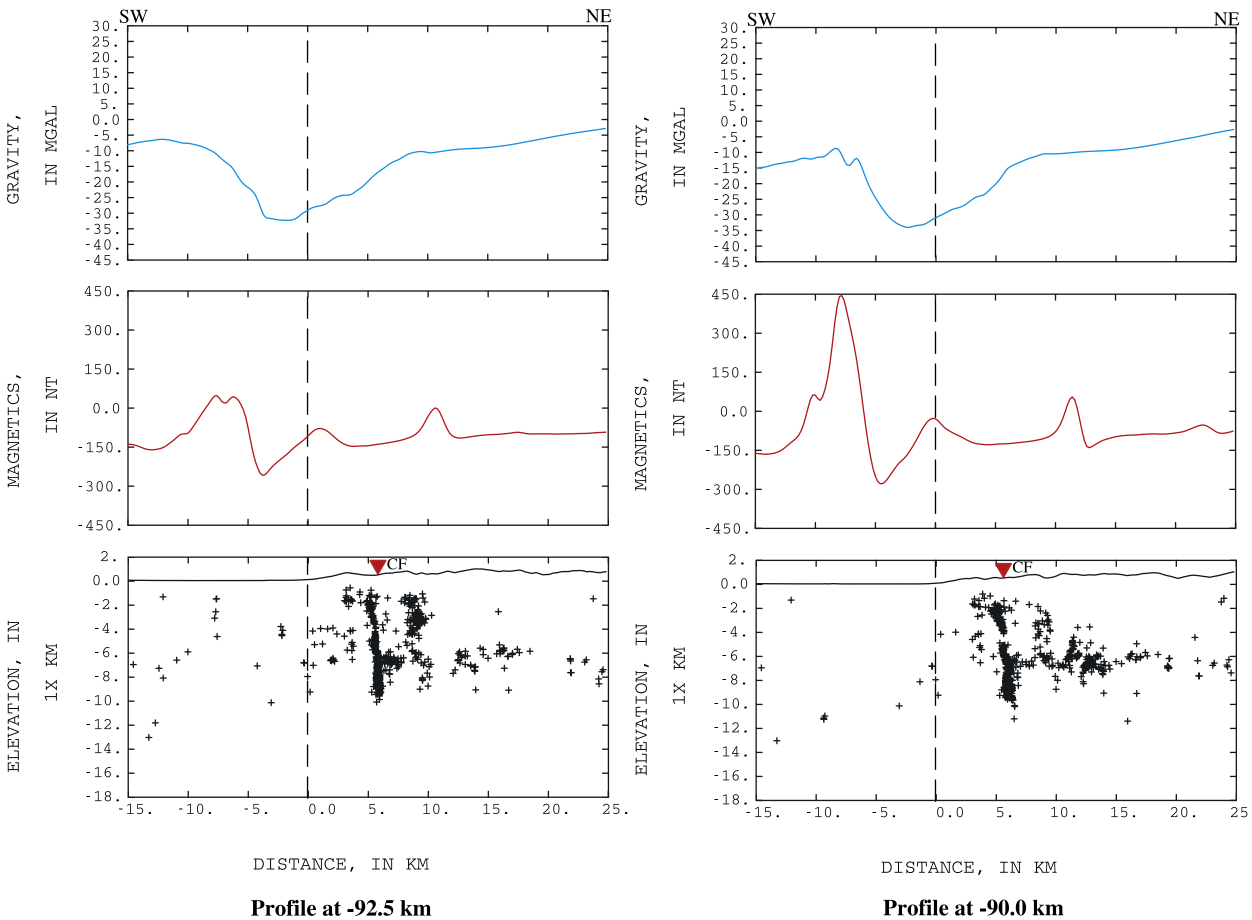

Figure A23. Gravity, magnetic, and seismicity data across the Hayward Fault.

10.1029/2003GC000684

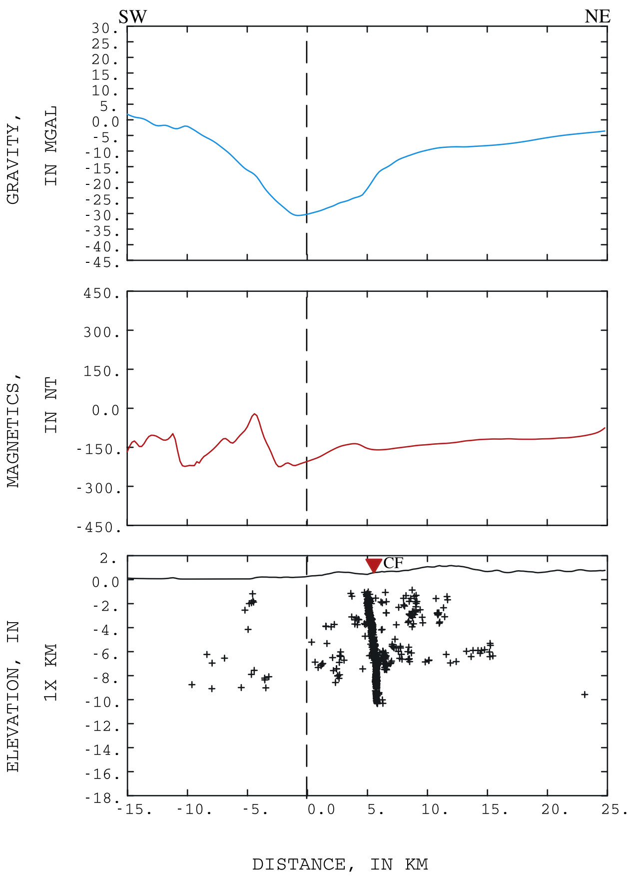

Profile at -97.5 km

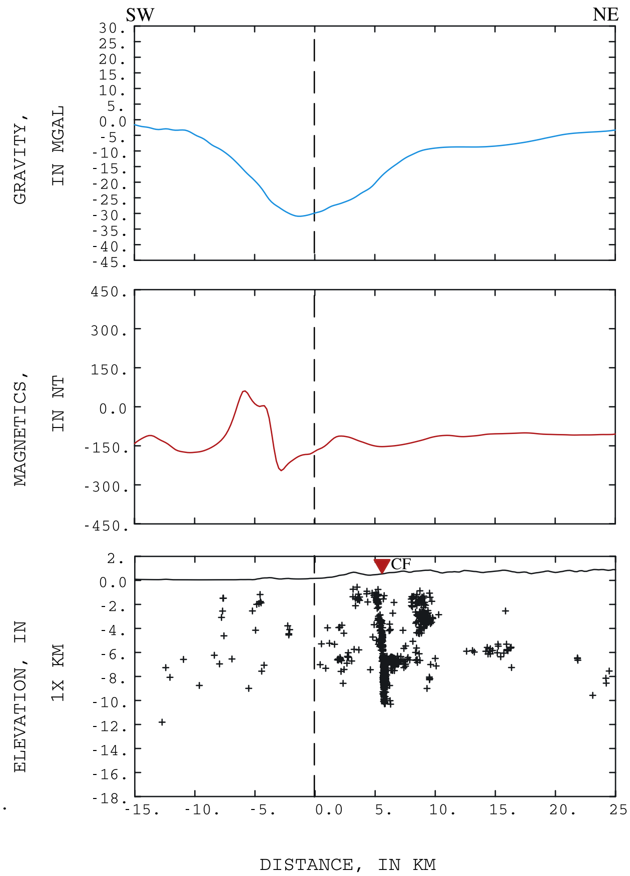

Profile at -95.0 km

Figure A24. Gravity, magnetic, and seismicity data across the Hayward Fault.

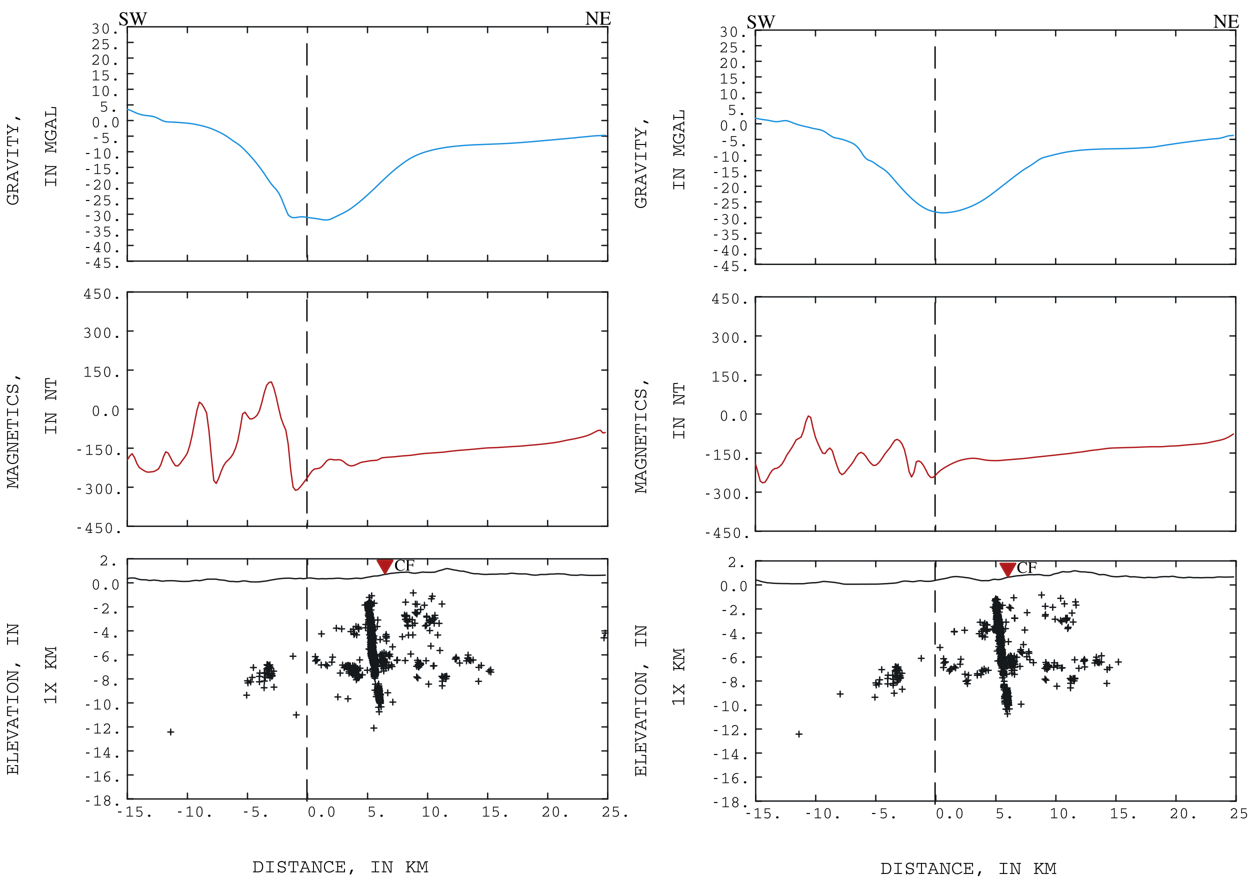

Profile at -102.5 km **Profile at -100.0 km**

Figure A25. Gravity, magnetic, and seismicity data across the Hayward Fault.

10.1029/2003GC000684

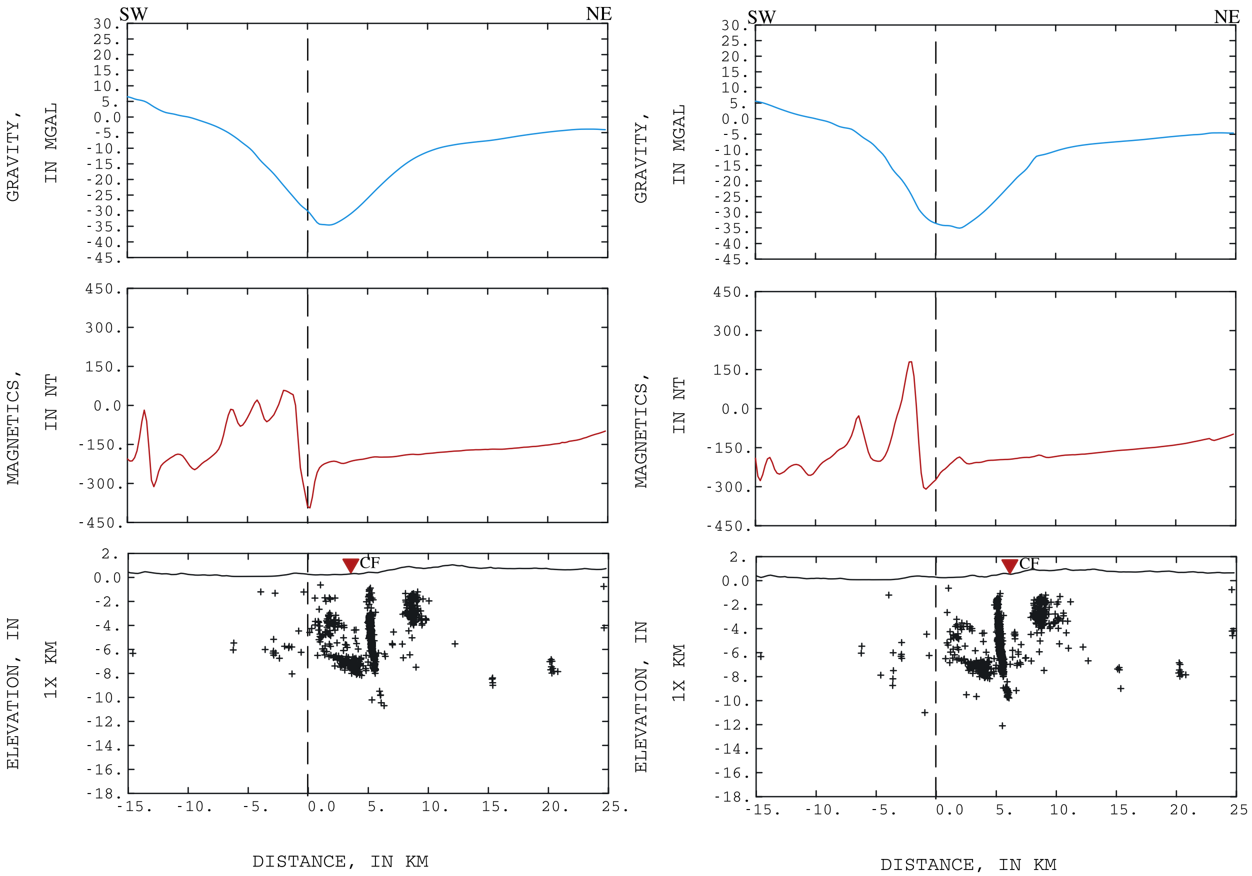

Profile at -107.5 km **Profile at -105.0 km**

Figure A26. Gravity, magnetic, and seismicity data across the Hayward Fault.

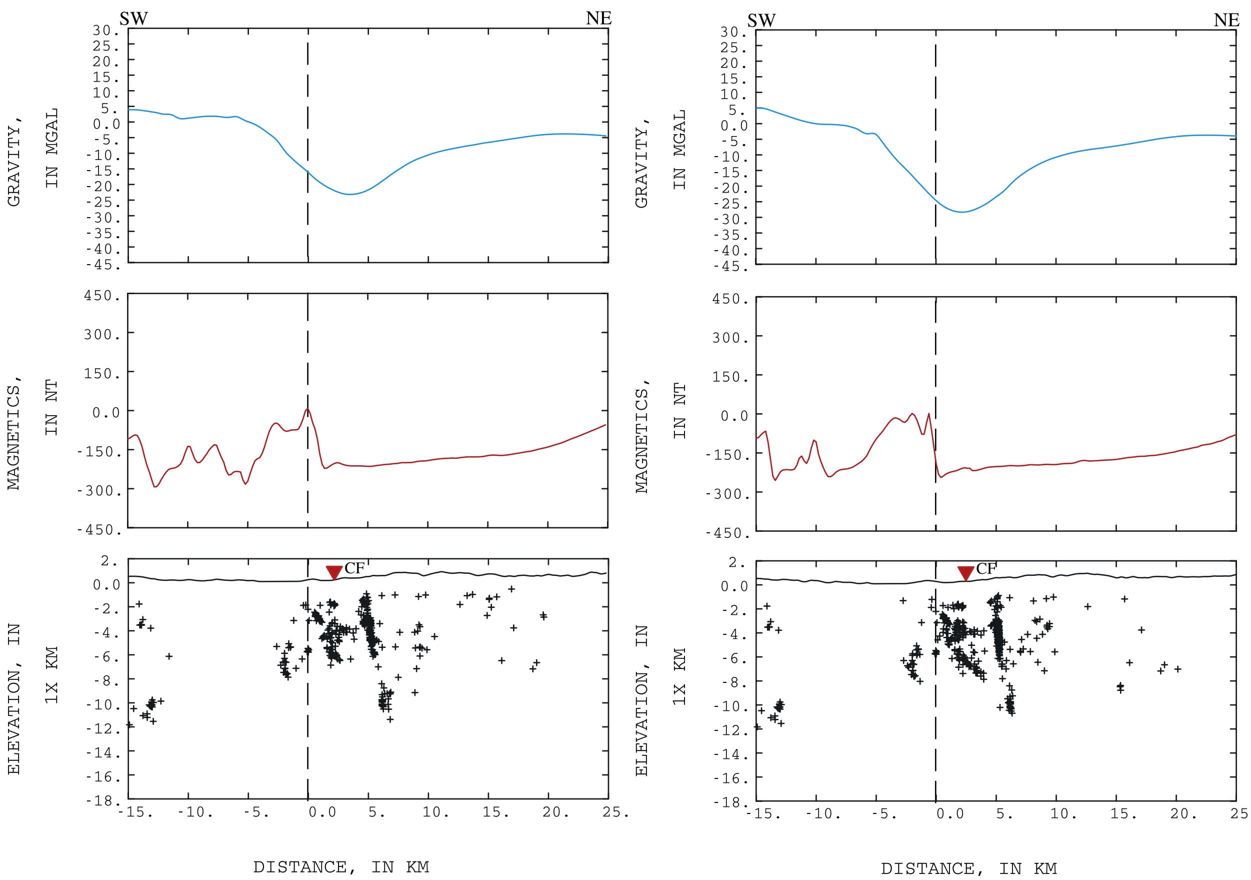

Profile at -112.5 km **Profile at -110.0 km**

Figure A27. Gravity, magnetic, and seismicity data across the Hayward Fault.

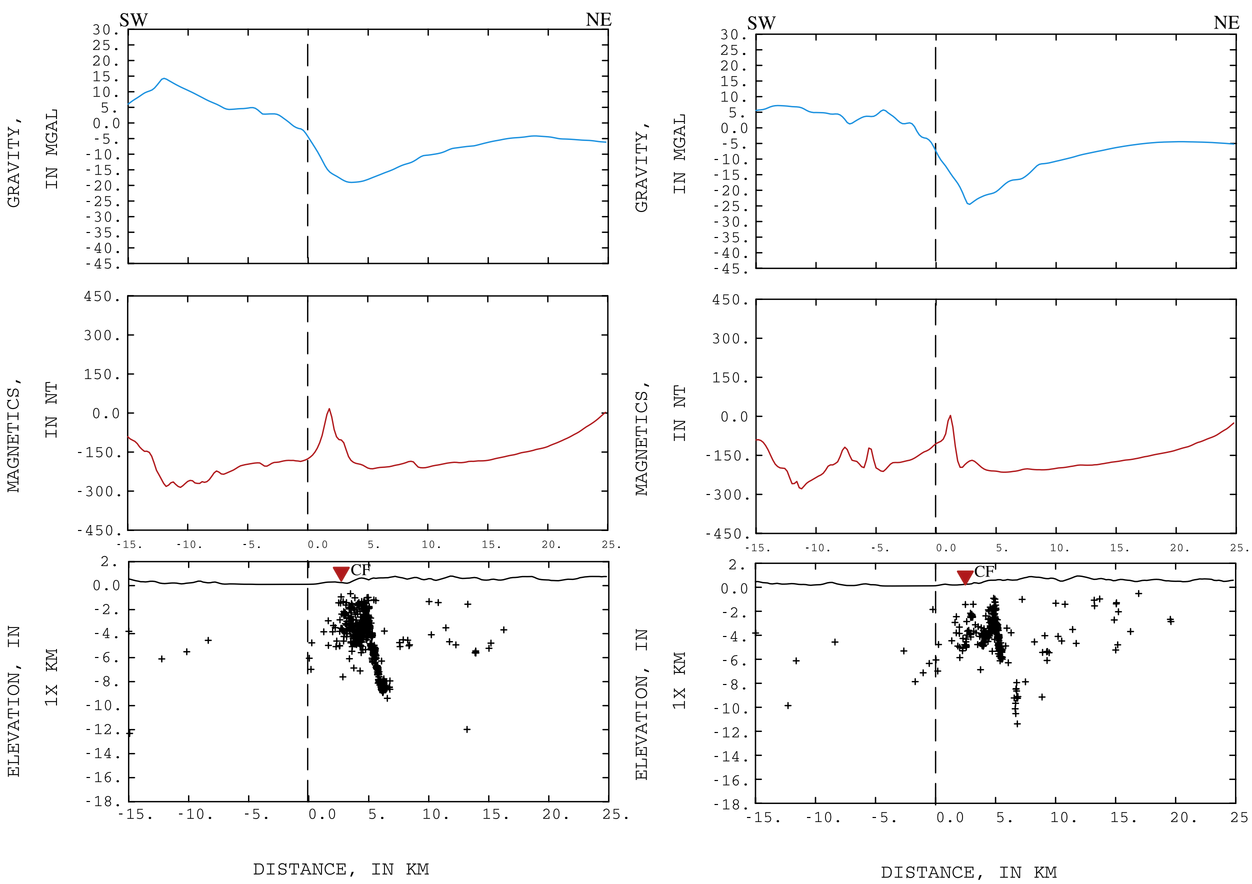

Profile at -117.5 km **Profile at -115.0 km**

Figure A28. Gravity, magnetic, and seismicity data across the Hayward Fault.

10.1029/2003GC000684

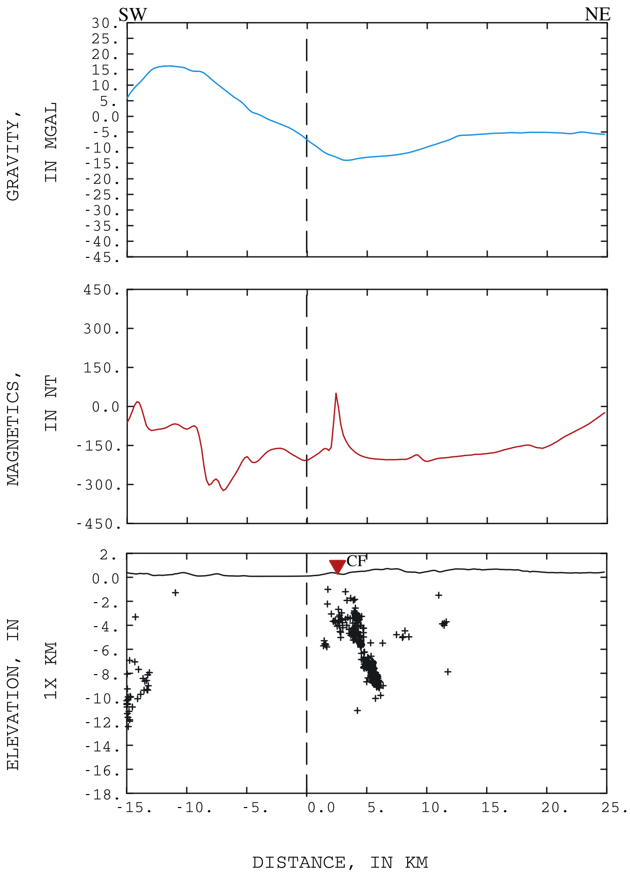

Profile at -122.5 km

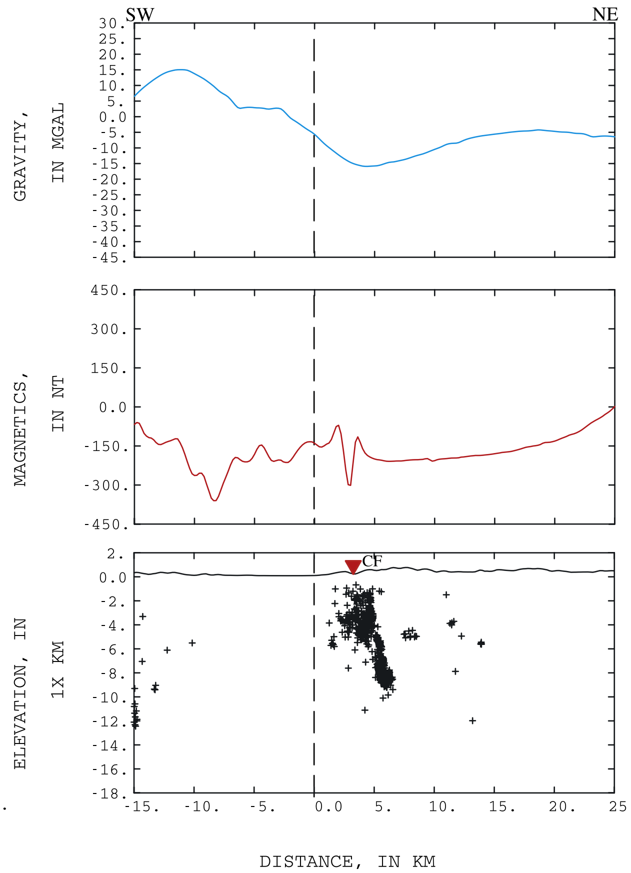

Profile at -120.0 km

Figure A29. Gravity, magnetic, and seismicity data across the Hayward Fault.

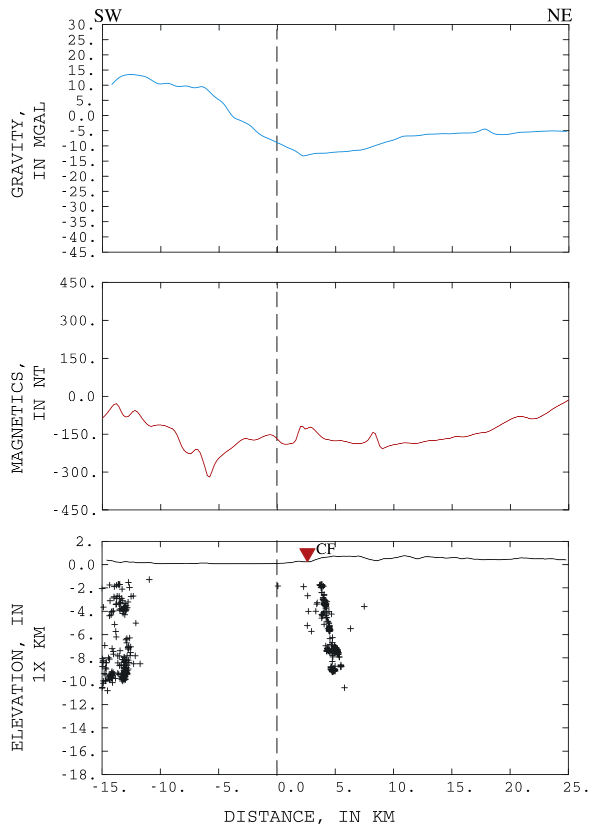

Figure A30. Gravity, magnetic, and seismicity data across the Hayward Fault.

[*Ponce et al.*, 2003a], and correlates with a bend in the active surface trace of the fault described by *Lienkaemper et al.* [1991].

3.3. Seismicity

[14] *Oppenheimer et al.* [1992] described the seismicity along the Hayward Fault on the basis of University of California data since 1910 and USGS data since 1969, *Bakun* [1999] described the seismic activity of the San Francisco Bay region, and *Waldhauser and Ellsworth* [2000, 2002] described the results of relocated hypocenters. Few recorded earthquakes along the Hayward Fault have reached magnitudes greater than about *M*4.5 (e.g., the October 2001, *M*4.5 El Cerrito earthquake). However, the Hayward Fault is the site of one of the largest historic earthquakes in the region—the October 1868, *M*6.8 earthquake. An 1836 earthquake (*M*6), previously thought to be on the Hayward Fault is now believed to have occurred on the San Andreas Fault, east of Monterey Bay [*Toppozada and Borchardt*, 1998].

[15] NCSN catalog data suggest that presently recorded seismicity along the Hayward Fault occurs in a series of clusters and that the Hayward Fault may dip to the east. However, apparent nonverticality of the hypocenters along the Hayward Fault could be an artifact of the one-dimensional linear velocity model used to locate hypocenters or other hypocenter mislocation errors [*Oppenheimer et al.*, 1992].

[16] Although the double-difference relocated hypocenters are regional in nature, they reveal that seismicity does indeed occur in a series of clusters with hypocenters that reach a depth of about 12 to 13 km. In general, relocated seismicity data, especially along the central and southern parts of the Hayward Fault, show increasing focal depths on the northeastern side and away from the fault, suggesting that the Hayward Fault dips to the northeast (Figure 4). Detailed cross sections of seismicity data (see Appendix A) indicate that the dip of the Hayward Fault may vary from near vertical in the northwestern part of the fault (profiles at −20 and −22.5 km), to about 75°NE at San Leandro in the central part of the fault (profiles at −32.5 and −37.5 km), to about 50°NE in the southeastern part of the fault (profiles at −80 and −82.5 km).

[17] Epicenters that follow and correlate to the surface trace of the Mission Fault (profiles −50 to −67.5), herein referred to as the Mission seismicity trend, are probably occurring on a steeply NE-dipping Hayward Fault plane at depth [see *Andrews et al.*, 1993; *Waldhauser and Ellsworth*, 2002; *Ponce et al.*, 2003b; *Simpson et al.*, 2003; *Manaker et al.*, 2004]. Relocated seismicity data suggest that above a 6 km depth the southern extension of the Hayward Fault may be connected in a structurally complex way to the central Calaveras Fault and that below about 6 km the connection may be less complex and involve near vertical fault segments forming a restraining bend along the Mission seismicity trend (profiles −72.5 to −87.5 km) [*Simpson et al.*, 2003].

[18] At the surface, and in the stepover region between the Hayward and Calaveras Faults, the southern extension of the mapped recent trace of the Hayward Fault (Figure 1) is parallel to the Calaveras Fault and forms a series of en echelon reverse and oblique faults with no apparent throughgoing connection with the Calaveras Fault. The connection between the Hayward

Table A1. Example Listing of Regional Relocated Double-Difference Hypocenters

Identifier	Longitude, °	Latitude, °	Depth, km	Magnitude	Year	Month	Day	Hour
17143	−121.63988	37.25925	6.7	2.5	1984	5	1	2
17150	−121.62807	37.24344	6.4	1.4	1984	5	1	3
17155	−121.65679	37.28623	10.0	0.8	1984	5	1	3
17156	−121.63922	37.25765	6.5	2.6	1984	5	1	4
17160	−121.65227	37.27337	6.0	1.4	1984	5	1	4
17164	−121.65208	37.22651	3.8	1.1	1984	5	1	6
17165	−121.68603	37.31436	6.4	0.7	1984	5	1	7
17171	−121.56002	37.15176	3.2	1.0	1984	5	1	7
17172	−121.52514	37.11036	5.6	0.8	1984	5	1	7
17180	−121.64542	37.2168	4.1	0.6	1984	5	1	9
17181	−121.65543	37.27731	6.1	0.4	1984	5	1	9
17186	−121.55232	37.1549	5.6	0.8	1984	5	1	11
17188	−121.65801	37.28045	6.2	1.9	1984	5	1	11
17190	−121.65385	37.28253	9.5	1.0	1984	5	1	11
17192	−121.63294	37.25964	9.8	0.7	1984	5	1	12
17193	−121.57224	37.15479	4.2	1.4	1984	5	1	13
17194	−121.59768	37.19545	3.4	1.4	1984	5	1	13
17195	−121.57352	37.15577	3.9	0.8	1984	5	1	13
17196	−121.5579	37.14826	3.6	1.4	1984	5	1	14
18768	−121.61432	37.22331	6.1	0.8	1984	5	1	14
18769	−121.62265	37.28401	3.6	0.6	1984	5	1	14
18775	−121.62316	37.28129	3.1	3.0	1984	5	1	15
18778	−121.56811	37.15615	3.9	1.6	1984	5	1	15
17214	−121.65217	37.27935	9.1	1.1	1984	5	1	16
17236	−121.64286	37.24294	8.1	1.3	1984	5	1	19
17237	−121.69913	37.33196	7.5	1.6	1984	5	1	19
18916	−121.6554	37.27792	6.5	0.9	1984	5	1	21
17245	−121.61751	37.2284	5.5	3.0	1984	5	1	23
17248	−121.69494	37.46745	2.7	1.8	1984	5	1	23
18920	−121.64869	37.27501	8.9	2.9	1984	5	2	4
18957	−121.6609	37.2177	6.5	1.7	1984	5	2	4
17407	−121.65694	37.28576	9.3	0.9	1984	5	2	5
18959	−121.66019	37.28371	6.6	2.1	1984	5	2	5
18964	−121.69048	37.32055	8.4	1.1	1984	5	2	5
17411	−121.62334	37.28245	3.0	0.9	1984	5	2	6
17270	−121.67129	37.3511	2.6	1.6	1984	5	2	7
17272	−121.6669	37.29026	6.0	1.7	1984	5	2	7

and Calaveras Faults appears to take place at depth, over a zone about 4 km wide and about 25 km long.

Appendix A

[19] Figures A1–A30 are gravity and magnetic profiles, and seismicity cross sections across the Hayward Fault. The origin is at Pinole Point. The profiles are spaced 2.5 km apart starting from 20 km northwest of Pinole Point to −125 km southeast of Pinole Point. The profiles are perpendicular to the Hayward Fault and extend 15 km southwest of and 25 km northeast of the fault for a total length of 40 km. Seismicity data are projected onto the profile line using a window of 2.5 km.

[20] The symbols and abbreviations are as follows: red triangles, approximate location of faults; CF, Calaveras Fault [*Jennings et al.*, 1977]; HF, recent trace of the Hayward Fault [*Lienkaemper et al.*, 1991]; MF, Mission Fault [*Jennings et al.*, 1977]; RCF Rodgers Creek Fault [*Jennings et al.*, 1977]; TF, Tolay Fault [*Jennings et al.*, 1977].

[21] Seismicity data (modified from *Ellsworth et al.* [2000]) are also available as auxiliary material[1] in a tab delimited text file that contains an identifier, longitude (in decimal degrees), latitude (in decimal degrees), depth (in kilo-

[1] Auxiliary material is available at ftp://ftp.agu.org/apend/gc/2003GC000684.

meters), earthquake magnitude, year, month, day, and hour. (See Table A1 for an example listing.)

Acknowledgments

[22] We would like to thank Bill Ellsworth (USGS) for permission to use the double-difference relocated seismicity data set [*Ellsworth et al.*, 2000]. Earlier versions of this article benefited from reviews by Darcy McPhee and Bob Morin, of the U.S. Geological Survey, and by Steve Bedrosian, an anonymous reviewer, and the editors of Geochemistry, Geophysics, and Geosystems.

References

Andrews, D. J., D. H. Oppenheimer, and J. J. Lienkaemper (1993), The Mission link between the Hayward and Calaveras faults, *J. Geophys. Res.*, *98*(B7), 12,083–12,095.

Bakun, W. H. (1999), Seismic activity of the San Francisco Bay region, *Bull. Seismol. Soc. Am.*, *89*(3), 764–784.

Blakely, R. J. (1995), *Potential Theory in Gravity and Magnetic Applications*, 441 pp., Cambridge Univ. Press, New York.

Bürgmann, R. D., D. Schmidt, R. M. Nadeau, M. d'Alessio, E. Fielding, D. Manaker, T. V. McEvilly, and M. H. Murray (2000), Earthquake potential along the northern Hayward fault, *Science*, *289*, 1178–1182.

Ellsworth, W. L., et al. (2000), Seismicity of the San Andreas Fault system in central California: Application of the double-difference location algorithm on regional scale, *Eos Trans. AGU*, *81*(48), Fall Meet. Suppl., Abstract S21D-01.

Graymer, R. W. (2000), Geologic map and map database of the Oakland metropolitan area, Alameda, Contra Costa, and San Francisco Counties, California, *U.S. Geol. Surv. Misc. Field Stud., Map MF-2342*, 29 pp., scale 1:50,000.

Graymer, R. W. (2003), Long-term history of the Hayward Fault Zone, in *Proceedings of the Hayward Fault Workshop, Eastern San Francisco Bay Area, California, September 19–20, 2003*, edited by D. A. Ponce et al., *U.S. Geol. Surv. Open File Rep.*, *03-485*, 14.

Graymer, R. W., A. M. Sarna-Wojcicki, J. P. Walker, R. J. McLaughlin, and R. J. Fleck (2002), Controls on timing and amount of right-lateral offset on the East Bay fault system, San Francisco Bay region, California, *Geol. Soc. Am. Bull.*, *114*(12), 1471–1479.

International Union of Geodesy and Geophysics (1971), *Geodetic Reference System 1967*, *Int. Assoc. Geod. Spec. Publ.*, *3*, 116 pp., Toronto, Canada.

Jachens, R. C., and C. W. Roberts (1981), Documentation of a FORTRAN program, 'isocomp', for computing isostatic residual gravity, *U.S. Geol. Surv. Open File Rep., 81-574*, 26 pp.

Jennings, C. W., R. G. Strand, and T. H. Rogers (1977), Geologic map of California, scale 1:750,000, Calif. Geol. Surv., Sacramento.

Langel, R. A. (1992), International geomagnetic reference field: The sixth generation, *J. Geomagn. Geoelectr.*, *44*(9), 679–707.

Lienkaemper, J. J., G. Borchardt, and M. Lisowski (1991), Historic creep rate and potential for seismic slip along the Hayward fault, California, *J. Geophys. Res.*, *96*(B11), 18,261–18,283.

Manaker, D. M., A. J. Michael, and R. D. Bürgmann (2004), Subsurface structure and mechanics of the Calaveras-Hayward Fault stepover from three-dimensional Vp and seismicity, San Francisco Bay region, California, *Bull. Seismol. Soc. Am.*, in press.

Marlow, M. S., R. C. Jachens, P. E. Hart, P. R. Carlson, R. J. Anima, and J. R. Childs (1999), Development of San Leandro synform and neotectonics of the San Francisco Bay block, California, *Mar. Pet. Geol.*, *16*, 431–442.

Morelli, C. (Ed.) (1974), *The International Gravity Standardization Net 1971*, *Int. Assoc. Geod. Spec. Publ., 4*, 194 pp., Int. Assoc. of Geod., Paris.

Oppenheimer, D. H., I. G. Wong, and F. W. Klein (1992), The seismicity of the Hayward fault, California, in *Proceedings of the Second Conference on Earthquake Hazards in the Eastern San Francisco Bay Area*, edited by G. Borchardt, et al., *Calif. Div. Mines Geol. Spec. Publ.*, *113*, 91–100, Calif. Geol. Surv., Sacramento.

Ponce, D. A. (2001), Principal facts for gravity data along the Hayward fault and vicinity, San Francisco Bay Area, northern California, *U.S. Geol. Surv. Open File Rep., 01-124*, 25 pp.

Ponce, D. A., T. G. Hildenbrand, and R. C. Jachens (2003a), Gravity and magnetic expression of the San Leandro gabbro with implications for the geometry and evolution of the Hayward Fault zone, northern California, *Bull. Seismol. Soc. Am.*, *93*(1), 14–26.

Ponce, D. A., G. A. Phelps, R. W. Graymer, R. C. Jachens, R. W. Simpson, and C. M. Wentworth (2003b), Geophysical anomalies and seismicity suggest a connection between the Hayward and Calaveras Faults, eastern San Francisco Bay Area, northern California, *Eos Trans. AGU*, *84*(47), Fall Meet. Suppl., Abstract T11D-0425.

Simpson, R. W. (2000), Watching the Hayward fault, *Science*, *289*, 1147–1148.

Simpson, R. W., R. W. Graymer, R. C. Jachens, D. A. Ponce, and C. M. Wentworth (2003), Structures in the Hayward and Calaveras Fault Zones from relocated seismicity, *Eos Trans. AGU*, *84*(47), Fall Meet. Suppl., Abstract T11D-0426.

Snyder, D. B., C. W. Roberts, R. W. Saltus, and R. F. Sikora (1981), Magnetic tape containing the principal facts of 64,402 gravity stations in the State of California, *U.S. Geological Survey Report, 2,161, PB82-168287*, 30 pp., Natl. Tech. Inf. Serv., U.S. Dept. of Commer., Springfield, Va.

Swick, C. A. (1942), Pendulum gravity measurements and isostatic reductions, *U.S. Coast Geod. Surv. Spec. Publ., 232*, 82 pp., U.S. Coast and Geod. Surv., Washington, D. C.

Toppozada, T. R., and G. Borchardt (1998), Re-evaluation of the 1836 "Hayward Fault" earthquake and the 1838 San Andreas Fault earthquake, *Bull. Seismol. Soc. Am.*, *88*, 140–159.

U.S. Geological Survey (1992), Aeromagnetic map of Livermore and vicinity, California, *U.S. Geol. Surv. Open File Rep., 92–531*.

U.S. Geological Survey (1996), Aeromagnetic map of the central San Francisco Bay area, California, *U.S. Geol. Surv. Open File Rep., 96–530*.

Waldhauser, F., and W. L. Ellsworth (2000), A double-difference earthquake location algorithm: Method and application to the northern Hayward fault, *Bull. Seismol. Soc. Am.*, *90*(6), 1353–1368.

Waldhauser, F., and W. L. Ellsworth (2002), Fault structure and mechanics of the Hayward Fault, California, from double-difference earthquake locations, *J. Geophys. Res.*, *107*(B3), 2054, doi:10.1029/2000JB000084.

Wolfe, C. J. (2002), On the mathematics of using difference operators to relocate earthquakes, *Bull. Seismol. Soc. Am.*, *92*(8), 2879–2892.

Working Group on California Earthquake Probabilities (1999), Earthquake probabilities in the San Francisco Bay region: 2000 to 2030—A summary of findings, *U.S. Geol. Surv. Open File Rep., 99–517*, 60 pp.

Working Group on California Earthquake Probabilities (2003), Earthquake probabilities in the San Francisco Bay region: 2002–2031, *U.S. Geol. Surv. Open File Rep., 03–214*, 235 pp.

Zhang, H., and C. H. Thurber (2003), Double-difference tomography: The method and its application to the Hayward Fault, California, *Bull. Seismol. Soc. Am.*, *93*(5), 1875–1889.